AN ABSTRACT OF THE THESIS OF

Sidi Lian for the degree of Master of Science in Materials Science presented on December 19, 2014.

Title: Heat Treatment Effects on CPM-M4 Tool Steel Performance as Edged Blade Material.

Abstract approved:

_____

Julie Tucker

CPM-M4 tool steel is a commonly used knife blade material due to its high strength and wear resistance. The goal of this thesis is to understand how heat treatment parameters affect blade performance and microstructure. Five heat treatments were applied to CPM-M4 steel by varying austenitizing and tempering temperatures. The microstructures were examined by optical microscopy, scanning electron microscopy and limited amounts of energy-dispersive X-ray spectroscopy. The carbide fraction, size, count, spacing and chemistry were characterized from the microstructural analysis. Blade performance was examined by hardness, 3-Point bend, impact, and CATRA (edge retention) testing. The results show that the austenitizing temperature is a significant factor that affects all mechanical properties tested. The max load in 3-Point bend test increases with the carbides fraction that can be maximized by controlling austenitizing temperature. Both austenitizing temperature and tempering temperature have significant effects on the hardness. As for the impact performance, the impact toughness increases with

the carbides density. Additionally, we can achieve comparatively high impact toughness in low austenitizing temperature without decreasing hardness through lowering the tempering temperature, because tempering temperature has no significant effect on impact toughness. The edge retention of CPM-M4 steel relates to its hardness. Harder materials can provide a better edge retention for knife blade.

HEAT TREATMENT EFFECTS ON CPM-M4 TOOL STEEL PERFORMANCE AS EDGED BLADE MATERIAL

by

Sidi Lian

A THESIS

submitted to

Oregon State University

in partial fulfillment of
the requirements for the
degree of

Master of Science

Presented December 19, 2014

Commencement June 2015

Master of Science thesis of Sidi Lian presented on December 19, 2014

APPROVED:

Major Professor, representing Materials Science

Director of the Materials Science Program

Dean of the Graduate School

I understand that my thesis will become part of the permanent collection of Oregon State University libraries. My signature below authorizes release of my thesis to any reader upon request.

Sidi Lian, Author

ACKNOWLEDGEMENTS

The author expresses sincere appreciation to Dr. Julie Tucker for her support and guidance as advisor, Dr. David Kim and Dr. Hector Vergara for their support as project advisors and contributions in this study, and Martin Mills, Gary Schuster and Dave Maxey for their technical support.

The author would also like to express personal appreciation to Bjorn Westman, Zach Terrell and Cody Fast.

TABLE OF CONTENTS

TABLE OF CONTENTS (Continued)

LIST OF FIGURES

LIST OF FIGURES (Continued)

LIST OF TABLES

Table Page

LIST OF APPENDIX FIGURES

LIST OF APPENDIX TABLES

LIST OF EQUATIONS

Equation Page

HEAT TREATMENT EFFECTS ON CPM-M4 TOOL STEEL PERFORMANCE AS EDGED BLADE MATERIAL

1 INTRODUCTION

The purpose of this project is to understand the effects of heat treatment parameters on the microstructure and performance of steel knife blades. Understanding this relationship will allow for the optimization of knife properties. Several characteristics of knife blades influence their performance, including cutting edge geometry, bevel geometry, blade profile, and the properties of the parent material, such as hardness, toughness and wear-resistance. Heat treatments are critical for improving the properties of the parent material. Different heat treatment parameters will result in different properties of the base materials. The heat treatment process must be optimized to achieve the best combination of properties for a given application. This work explores the role of austenitizing and tempering temperatures on knife blade performance for alloy CPM-M4.

CPM-M4 is a high speed tool steel produced by powder-metallurgy. CPM-M4 has high vanadium, molybdenum and tungsten content, which provide good wear-resistance and cutting edge stability [1]. M4 is also known for having a good combination of hardness and toughness. The chemical composition of CPM-M4 used in this study and the AISI-M4 composition are shown in Table 1.

Table 1. Chemical composition of CPM-M4 steel (in weight percent)

	C	Cr	Mn	Mo	P	S	Si	V	W	Fe
CPM-M4*	**1.45**	**4.02**	**0.3**	**5.11**	**0.019**	**0.063**	**0.52**	**3.89**	**5.41**	**Bal.**
AISI-M4	**1.25-1.40**	**3.75-4.75**	**0.15-0.40**	**4.25-5.50**	**0.03 Max**	**0.03 Max**	**0.20-0.45**	**3.75-4.50**	**5.25-6.50**	**Bal.**

*Independent chemical analysis ASTM standards E415-14 and E1019-11

A series heat treatments are performed in order to optimize CPM-M4 for knife blade performance. Austenitizing, quenching and tempering are the three major steps of the heat treatment process. There are many parameters that can be controlled for each of these steps including temperature, time and media. Austenitizing is a high temperature heat treatment performed to transform the room temperature microstructure (ferrite+pearlite) to austenite. During this phase transformation, carbides are dissolved and distributed in the austenite matrix. Following austenization, the material is rapidly cooled (quenching) to transform the matrix into martensite, which is a hard, brittle phase. Toughness is returned to the material by tempering at an intermediate temperature. During tempering the martensite phase is transformed into tempered martensite and carbides can nucleate and grow. In this study, the austenitizing and tempering temperature were varied while all other parameters were held constant. The resulting microstructure of the heat treated steels was examined by Optical Microscopy, Scanning Electron Microscopy (SEM) and Energy-dispersive X-ray spectroscopy (EDX). The average size, distribution and fraction of carbides were analyzed by statistical methods and the alloy content of different phases was defined by element analysis.

Differences in microstructures will affect knife blade performance. In order to correlate microstructure to mechanical properties, several tests were performed including: Rockwell C hardness test, 3-point bend fracture toughness test, impact toughness test, and CATRA cutting edge stability test. The results from mechanical testing and microstructure examination help relate heat treating parameters to the knife blade performance. This understanding will guide future heat treatments to fully optimize M4 in this application.

The rest of the thesis is organized as follows: Chapter 2 introduces the background through the literature review. Chapter 3 describes the experiment design of this study. In Chapter 4, the experiment execution is described, including the procedures of the microstructure analysis and the performance tests. The results are presented in Chapter 5, then a discussion of the results is given in Chapter 6. Chapter 7 and 8 state the conclusions drawn from this study and the possible future work.

2 REVIEW OF LITERATURE

2.1 INTRODUCTION

In this chapter, the background of the Powder-Metallurgy process is presented first, to explain how the process changes the material's properties and microstructure. Then, the literature based on the continuous cooling transformation (CCT) diagram of M4 steel is reviewed to describe the heat treatment processes. Next, the basic principles of heat treatment processes are presented and recommended heat treatment practices are discussed. Finally, the wear-resistance of M4 steel is discussed.

2.2 POWDER METALLURGY

In addition to adjusting alloy content and applying specific heat treatments to improve steels, different manufacturing techniques are employed to lower cost and improve performance. Powder metallurgy (PM) is one of these techniques that is applied in CPM-M4 steel. PM is an alternative method of producing steel, it is based on compacting the metal powder into specific shapes under high temperature and pressure [2], [3]. The PM process provides fine carbide sizes and uniform carbides distribution resulting in good dimensional stability and toughness.

Humans have thousands of years of experience in the PM method, which can be traced back to ancient Egypt [3]. From the second half of the 20th century, PM has been a popular and important method in modern steel industry. As for practical applications of PM , Randall M. German (1998) introduced two

extreme methods in his book [3]. One method is to densify the metal powders in sintering, while the other is a pressing process. In industry, different companies apply their own processes between these two extremes [3].

The PM method has many advantages. It is easier to shape materials into more complex components with PM as compared to traditional methods. Additionally, the PM process also makes the microstructure of the final product more controllable, which usually provides a fine and uniform carbides distribution. Therefore, PM methods have been a popular practice in modern steel manufacturing.

To achieve optimal performance of CPM-M4, a proper selection of heat treatment parameters is required. In this study, we will focus on the effect of heat treatment on mechanical properties. The relationship between specific heat treatments and the resulting microstructures will be analyzed. The continuous cooling transformation (CCT) diagram is a useful tool for selecting heat treatment parameters.

2.3 CCT DIAGRAM OF M4 STEEL

From a data sheet of Erasteel Company [4], a rough CCT diagram shows the martensite transformation start temperature (M_s temperature) at around 300°F (150°C). The CCT diagram is presented in Figure 1. The general areas of austenite, bainite, pearlite and martensite are shown in the diagram.

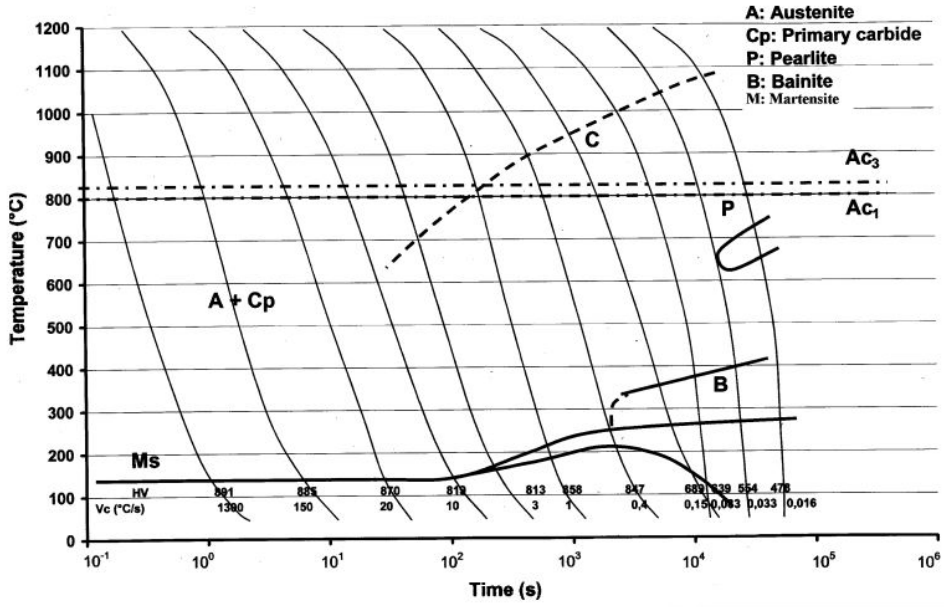

Figure 1. The continuous cooling transformation diagram for AISI M4 tool steel [4]

To develop a more accurate CCT diagram for M4 steel, Briki (2007) [5] performed a study based on the new evolution of the dilatometric method. In recent years, the dilatometric method has been improved significantly, which provides a more sensitive and precise way to detect the transformation during the cooling process of even some minor transformations [6]. In their experiment, M4 steel was austenitized at 2228°F, than cooled at different cooling rates from 32.013°F/s to 392°F/s. Two dilatometers, DI24 and DT1000 were used to detect the dimensional changes in the experiment. By using scanning electron microscopy and energy-spectrum analysis, the microstructure showed the gray color V-rich carbides with size of 10-15μm and the white color W-rich carbides with size of 1-5μm before austenitizing. The $M_{23}C_6$ carbides were dissolved at 1922°F, while the M_6C and MC carbides were dissolved at higher than 2228°F. Therefore, carbides would be partially dissolved during austenitizing at 2228°F.

Dilatometric curves under different cooling rates were plotted after the cooling process. Phase transformations can be determined by derivative curves. In fast cooling rate (greater than 59°F/s) condition, the M_s temperature was identified at 374°F and the M_f (martensite transformation finish) temperature at -130°F, when samples were cooled in liquid nitrogen. However, a quite low M_f temperature would lead to an incomplete martensite transformation with a large volume of retained austenite [7]. In this case, there was about 15% retained austenite in as-quenched condition. In a medium cooling rate (from 32.36°F/s to 59°F/s), a splitting phenomena happened that resulted in two M_s temperatures. The first M_s temperature ranges from 392°F to 788°F by decreasing the cooling rate from 59°F/s to 32.36°F/s. The retained austenite was less for the fast cooling rate, since the M_f temperature was increased to a relative high temperature. When the cooling rate was slower than 33.8°F/s, the M_f temperature was detected at greater than 194°F. In a slow cooling rate (slower than 32.36°F/s), bainite, pearlite and ferrite were formed instead of austenite-martensite transformation. The new CCT diagram for M4 steel is shown in Figure 2. According to their study about the M4 CCT diagram, a medium cooling rate should be applied to achieve less retained austenite and more carbides precipitation [5], [6], [8].

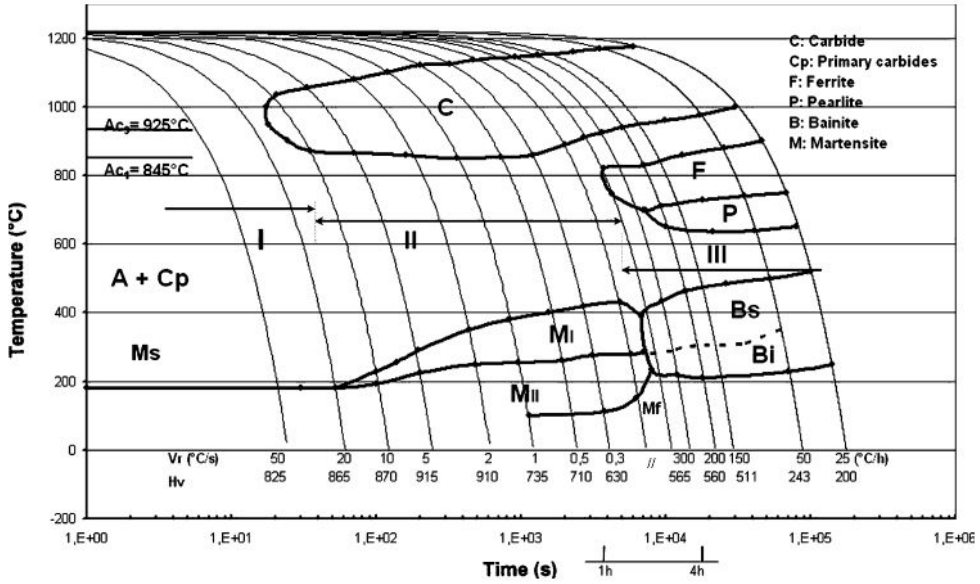

Figure 2. CCT diagram for M4 steel austenitized at 1220°C [5]

On the basis of the CCT diagram for M4 steel and the specific properties needed for tool steels, some guidelines for heat treatment practices have been developed. The following section discusses the common heat treatment practices for M4.

2.4 HEAT TREATMENT PRACTICE

As a significant part of metallurgy, many studies have been performed in the area of steel heat treating. Generally, steel heat treatments consist of austenitizing, quenching and tempering. Each step plays its own role in developing the microstructure and properties of a steel, however, they can also affect or cooperate with each other.

Austenite is a solid solution of carbon and alloy elements in γ-iron, which has the face-centered cubic (F.C.C.) crystal structure. The process of a plain carbon steel forming single-phase austenite, when heated above a critical

temperature for a long time, is called *austenitizing* [2]. The austenite transformation temperature is where pure iron change from the body-centered cubic (B.C.C) crystal structure to F.C.C upon heating [2].

Due to the F.C.C structure, austenite can accommodate a higher solubility of carbon. Krauss (1980) explained the better carbon solubility in F.C.C structure. In B.C.C and F.C.C crystal structures, there are two kinds of interstitial sites, octahedral and tetrahedral . In octahedral sites, there are 6 nearest neighbor atoms, and there are 4 for the tetrahedral site. According the lattice parameter and geometry in F.C.C austenite, an atom 0.052nm in radius can be accommodated in an octahedral site and an atom 0.028nm in radius can fill a tetrahedral site. However in ferrite, a B.C.C structure, the atom radius is only 0.019nm in octahedral site and 0.035nm in tetrahedral site. Obviously, the austenite structure can provide more room for carbon atoms in octahedral site, although some expansion is needed since the carbon atom have a radius of 0.07nm [9].

In plain carbon steel, the austenitizing temperature ranges from 723°C to 1493°C according to the percentage of carbon content. It's a very large temperature range, so a proper temperature selection is important in this process. For high alloy steels, the increased amount of alloy elements form stable carbides, which need to be dissolved by increasing the austenitizing temperature [2]. Thelning said that most alloy elements increase the austenite transformation temperature except some austenite-formers like Ni and Mn [10]. More alloy elements dissolved in the matrix usually results in a more

uniform carbide distribution after tempering. For M4 steel, a relatively high austenitizing temperature should be applied because of its high alloy element contents. All of the alloy elements in M4, such as chromium, vanandium, molybdenum and tungsten, increase the austenitizing temperature. However, most of the alloy elements depress the start temperature martensite transformation when they dissolve in the iron matrix, which causes difficulty in the next process, quenching. A lower martensite start temperature will increase the higher content of austenite retained after quenching. Therefore, proper temperature selection is important for achieving specific properties [2].

For M4 steel, most practices [1,2,11,12] recommend an austenitizing temperature in the range between 2150°F and 2250°F for cutting-tool application. In this temperature range, a relatively high tempered hardness, which is between 64.5 HRC to 67 HRC, can be achieved. In Crucible Datasheet [1], austenitizing between 1875°F-2125°F is recommended for cold-working tools. However, ZAPP Materials Engineering [13] gives its recommendation of 2080°F-2150°F as the austenitizing temperature for cutting-tools and 1950°F-2050°F for cold-working tools, which require a higher toughness.

The other objective of the austenitizing process is to form martensite, which can only be produced from austenite. To achieve the martensite transformation, a quenching process should be applied following austenitizing.

Martensite is a metastable phase formed when an extremely fast cooling rate is applied to the austenite phase. It preserves the carbon content of the original

austenite. So it can be considered as ferrite in a supersaturate condition [14]. Therefore, the tetragonal distortion caused by the supersaturate carbon leads to a body-centered tetragonal (B.C.T) crystal structure of martensite. Because of the B.C.T structure, martensite has much higher hardness than any other phases.

T_e is the metastable equilibrium temperature for martensite. However, a lower temperature is required to provide enough driving force for the martensite transformation. This temperature is also called martensite transformation start temperature, Ms [14]. The final temperature in the quenching process should reach to at least M_s. To get a full transformation, another critical temperature, M_f (martensite finish), should be reached. However, there also retains some austenite content even when the cooling reach to M_f.

Obviously, determining the M_s and M_f temperatures is extremely important in the quenching process. Generally, the M_s and M_f temperatures depend on the alloy elements in the steel. Most of alloy elements decrease both M_s and M_f temperatures [2,14].

To avoid forming other phases such like bainite and pearlite, the cooling rate should be kept as fast as possible in the quenching process. However, the cooling rate is usually limited to the possible distortion or cracking during the transformation. To some extent, the additional alloy elements can deal with this problem. That means that the high-alloy steel can bear a faster cooling rate, which could lead to a fully martensite transformation.

Quenching media also plays an important role. A proper media can provide a stronger and uniform driving force that will affect the microstructure and the mechanical properties of the final product. In general, salt bath or oil quenching to 1000°F then air quenching to below 125°F is stated in most of the datasheets for M4 steel. For small materials, air quenching to 125°F directly is also reasonable. However, it cannot be applied on large materials, because it cannot provide a uniform cooling rate and may lead to distortion or cracking [1,12,13].

Although martensite is hard, it is not a desirable material in most manufacture applications because, a low ductility accompanies the high hardness. As knife steel, martensite is too fragile to be selected as the final structure. As Wilson [2] stated in his book: “as-quenched martensite should never be in the final structure.” A tempering process will help to soften the martensite by removing the tetragonal distortion and facilitating the precipitation of carbides.

Tempering at different temperatures will result in different stages of the phase transformation and different properties will be achieved. Let’s assume the tempering temperature starts from 32°F. At the beginning, the hardness will be increased slightly due to the formation of some thin carbide plate [2]. A maximum hardness will be achieved at 212°F for plain carbon steel accompanying with the formation of ε carbides. However, Madeleine also mentioned the temperature range for these carbides as 122°F-320°F [14]. Generally, tempering below 482°F will lead to a good combination of hardness and toughness, due to the offset of increasing hardness by carbides

precipitation and increasing toughness by transforming martensite to tempered-martensite. When the temperature stays between 482°F-752°F, the modification of tetragonal distortion will be increased significantly and lead to a significant drop in hardness. However, toughness cannot be increased significantly at this temperature range because a phenomenon called 500°F temper brittleness. Wilson stated two reasons for this phenomenon. First reason is that the retained austenite-bainite transformation results in a loss of toughness, due to the brittleness of the bainite structure. Carbides also play an important role in this case. The carbides precipitate in grain boundaries making it more brittle [2]. In this aspect, some metallurgists also mentioned that the formation of orthorhombic carbides, Fe_3C is the reason of temper brittleness [15]. After that, a significant drop in hardness and increase in toughness will happen when the temperature stays between 698°F-1247°F [2].

Choosing the tempering temperature properly will decide what kind of properties are achieved in the final product. The alloying elements should be considered when deciding the tempering temperature. Most elements will retard the soften rate. That means a higher temperature is required when given properties should be achieved [2]. At higher temperatures, the alloy carbides will substitute for the Fe_3C carbides that usually leads to an increasing in hardness called secondary hardening [14]. As for temper brittleness, to some extent, elements like molybdenum eliminate this phenomenon because they will not precipitate in grain boundaries as carbides.

Multiple tempering steps are required for M4 steel. The maximum hardness can be achieved at 980°F due to the secondary hardening [2, 11, 12]. For better toughness, tempering at 1000°F to 1100°F is most generally recommended [1,2, 11-13].

Although there are many heat treatment recommendations, the specific parameters should be selected by the specific properties required. For M4 steel, good wear-resistance is its characteristic mechanical property. Therefore, some research focusing on the wear-resistance of M4 had been studied and will be discussed in the next section.

2.5 WEAR-RESISTANCE

Wear-resistance can be divided into two kinds of wear-resistance, adhesive and abrasive. M4 has excellent performance in both situations. To better understand wear performance, Fontalvo [16] performed a study to correlate the microstructure to the wear performance. In his study, carbides are the focus of the microstructural analysis. There were 6 alloys studied. M4 steel is the basic alloy, while the other 5 alloys have carbide content range from 0-25% in 5% increments. To keep the same composition and microstructure of the after-tempered martensite matrix, the compositions were simulated by the software Thermo-Calc and heat treatment parameters were decided by both Thermo-Calc and a dilatometer. Then, the only variable value is the carbides content and distribution. A Ball-on-Disk experiment was used in his study and the wear performances were compared with each other by using the volume of transfer materials. From the experiment results and microstructure analysis,

both carbides content and distance between carbides were concluded as the main parameters determining the adhesive wear performance. Higher carbides content and smaller distance between carbides can improve the adhesive wear performance [16].

As for abrasive wear performance, Wang [17] also mentioned M4 in his study. D2 steel was selected as the reference material in this experiment. Five kinds of steel powders clad on the substrate materials, AISI 1070 carbon steel. M4 powder is one of them. A Falex dry sand wheel test machine was applied in the abrasive wear test. The mass loss was calculated to compare the abrasive wear resistance. After comparing the abrasive behavior and the analysis of microstructures, both carbides and matrix microstructures were confirmed as determining factors in abrasive wear resistance of these steels, including M4 steel. Although the Mo-rich and W-rich carbides in M4 steel were harder than the chromium carbides in D2 steel, the abrasive resistance of M4 was inferior to D2 due to the tiny size of Mo-rich and W-rich carbides. However, in the comparison between M4 and CPM 10V steel, CPM 10V had better abrasive behavior due to harder V-rich carbides and larger volume fraction of carbides content, although the carbides sizes are comparable between CPM 10V and M4 [17].

2.6 SUMMARY

By reviewing of literature, we can clarify that a tempered-martensite matrix with fine size and uniform distributed carbides would be the desirable microstructure of CPM-M4 tool steel. According to the CCT diagram of M4

steel, a medium cooling rate (from 32.36°F/s to 59°F/s) should be applied. The heat treatment practices are fairly common from different sources, austenitizing around 2100°F, air quenching to 125°F and multiple tempering steps between 1000°F and 1100°F are recommended. Excellent wear-resistance is a characteristic property of CPM-M4 steel. Higher carbides content and smaller carbide distances improve the adhesive wear performance [16]. The carbides size and type affects the abrasive-wear resistance [17].

From the studies discussed above, some relationships between microstructures and wear resistance were investigated. The other mechanical properties are just mentioned on their values or given a general explanation in most of the reviewed literature. There is a lack of studies based on specific heat treatments for M4 steel. Most articles in the literature just state recommendations. Some mention the relationships between heat treatment parameters and the mechanical properties. However, microstructure, the bridge between heat treatment and mechanical performance, should be investigated comprehensively, quantitatively and with a sound scientific method.

3 EXPERIMENT DESIGN

3.1 OBJECTIVES AND REQUIREMENTS OF THE EXPERIMENT

The objective of this project is to relate heat treatment parameters to the microstructure and knife blade performance for CPM-M4 steel. The objectives of the experiment are shown schematically in Figure 3. The characteristic microstructure of the steel can be achieved by a specific heat treatment. Additionally, the edged blade performance also corresponds to the characteristic microstructure. Therefore, the microstructural analysis can be seen as a bridge in this study. To figure out how heat treatment affects the edged blade performance, the characteristic microstructure should be analyzed.

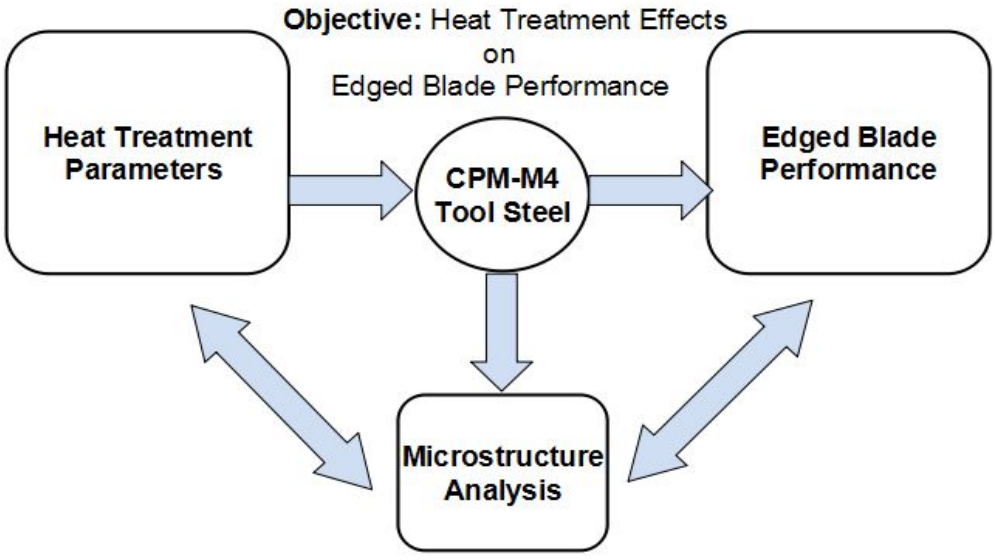

Figure 3. Objectives of experiment design

Controlling the heat treatment parameters is the key point in the experimental design. When a parameter is changed, all other parameters should remain

fixed, since different heat treatment parameters usually affect each other in the heat treatment process. Then the comparison between the heat treatments is based on a single parameter. As for the variation range, we will select a proper range according to two objectives. First, it should be in a reasonable range for austenitizing and tempering. For example, a good balance of hardness and toughness should be achieved for knife blade materials, so it's impractical if the tempering temperature is too low. On the other hand, to avoid the effects from uncontrollable factors, the parameters under control should achieve a significant difference in both the performance test and microstructure analysis.

For the performance tests, each test should be kept consistent to avoid the effects from uncontrollable noise factors. A testing procedure should be standardized for each performance test. The standard testing procedures are shown in the later chapter. To decide which kind of performance should be tested, a functional principle should be applied. Only properties relating to the edged blade performance are to be tested in this study.

The characteristic features of microstructure should be quantified. To get valid data and analysis results, the data collecting procedures should be kept consistent and the data analysis procedures should be appropriate.

3.2 HEAT TREATMENT PARAMETERS

According to the objectives and requirements of the experimental design, the matrix of heat treatment parameters is shown in Table 2. Two parameters are controlled in the experiment, austenitizing temperature and tempering temperature. The parameters marked in red color represent the the center point

of the experiment design (austenitized at 2100°F and double tempered at 1025°F). Additionally, a higher and lower parameter are applied for both processes, which are 2000°F and 2200°F for austenitizing and 925°F and 1125°F for tempering. Then, four different heat treatments are selected by combining the two parameters for each of the two processes. The experimental design generates a 2x2 matrix with a center point. The corners make a set of single variable experiments while the center point helps to explain coupled effects. To achieve full carbides participation and retained austenite transformation, double-temper is applied for the tempering process. The double temper is denoted by (X2) in Table 2.

Table 2. Heat treatment controlling matrix for CPM-M4 steel

Aust Temp (°F)	Temper Temp (°F)	Aust Temp (°F)	Temper Temp (°F)	Aust Temp (°F)	Temper Temp (°F)
2000	925 *X2*			2000	1125 *X2*
		2100	1025 *X2*		
2200	925 *X2*			2200	1125 *X2*

The austenitizing and tempering processes will affect both microstructure and material performance significantly. Temperature and time are the two factors for each process, which means the processes are easier to control and compare. Although quenching is also an important heat treatment process, it's much more complex to control. Many factors will affect the quenching process, such

as cooling rate, quenching media, sample dimensions and equipment. We use a consistent quenching process in our experiment. All of the heat treatment samples are quenched to below 125°F in nitrogen gas (at a medium quenching rate). Then the samples will be frozen at -120°F for 2 hours. The M_s temperature for M4 is between 392°F and 788°F and M_f temperature is around 194°F under a medium-cooling rate. Therefore the quenching process we use can achieve a full martensite transformation.

The holding time of tempering and austenitizing is related to temperature. In general, lower temperatures need longer holding time to achieve similar performance. The effect of tempering time and temperature is shown in Figure 4 [11]. Figure 4 shows the tempering temperature is more effective as compared to the holding time. For austenitizing, the time-temperature relationship is similar. The austenitizing process is less sensitive to time than to temperature. When the austenitizing temperature reaches a relatively high range, there is a negligible affect caused by changing the holding time. In this study, both austenitizing and tempering time are held constant, which are 30 minutes for austenitizing and 120 minutes for each of the double tempering processes.

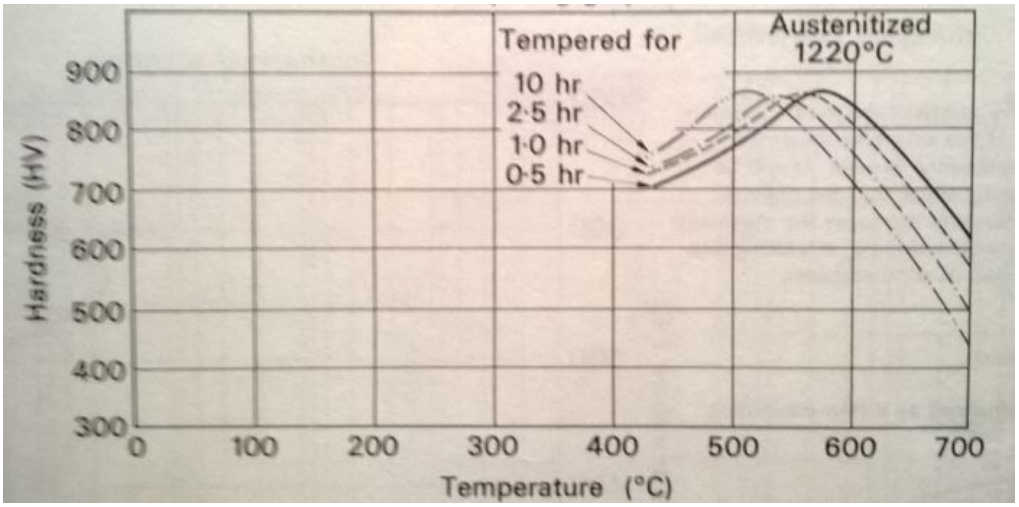

Figure 4. The effect of tempering temperature and time for M4 steel [11]

According to the literature and different datasheets for CPM-M4 steel heat treatments, austenitizing at 1950°F-2250°F is applicable for CPM-M4 steel. As for tempering temperature, 1000°F-1100°F are commonly recommended to balance hardness and toughness, which is a little higher than the secondary hardening temperature range (around 980°F). The center heat treatment in the experimental design (austenizing at 2100°F, temper at 1025°F) is in agreement with the recommendations from most of the reviewed literature. To generate a significant difference in microstructure and blade performance and still obtain practical properties for knife blade materials, ±100°F can be applied as a proper range of temperature change for both austenizing and tempering.

In the following chapters, five different heat treatments will be represented by A-T-, A-T+, center, A+T-, A+T+. “A” represents austenitizing, “T” represents tempering, “-” represents lower temperature, “+” represents higher temperature, “center” represents the center heat treatment parameters.

The experiment will be executed to apply the five different heat treatments as shown in Table 2. Eighty (80) samples were heat treated at the same time for each heat treatment. To better understand the role of the two heat treatment processes on the microstructure, as-quenched samples were also prepared after the three austenitizing treatments (2000°F, 2100°F, 2200°F).

For edge performance testing, hardness, toughness and cutting edge stability were selected as the representative properties of M4 steel. Also, the quantified microstructural analysis will focus on carbides fraction, size, count and distribution.

4 EXPERIMENT EXECUTION

4.1 SAMPLE PREPARATION FOR MICROSTRUCTURE EXAMINATION

4.1.1 Introduction

The first step in microstructural analysis is preparing the steel specimen so that distinct microstructure features (phases, grains) can be examined by both optical microscope and scanning electron microscope (SEM).

Different materials require specific preparation procedures. Five heat treatments were applied on CPM-M4 steel in this study. However, they all have similar features such as high hardness, identical alloy composition, and after heat treating their microstructures consists of tempered martensite and a variety of carbides. Therefore, the same sample preparation procedure can be used with the different heat treatments specimens studied.

4.1.2 Standard Preparation Procedures

Four procedures are applied to prepare specimens for SEM imaging: Sectioning, Mounting, Grinding and Polishing, and Etching (see details in Appendix 3). Figure 5 shows a summary of the different steps needed for specimen preparation for SEM imaging.

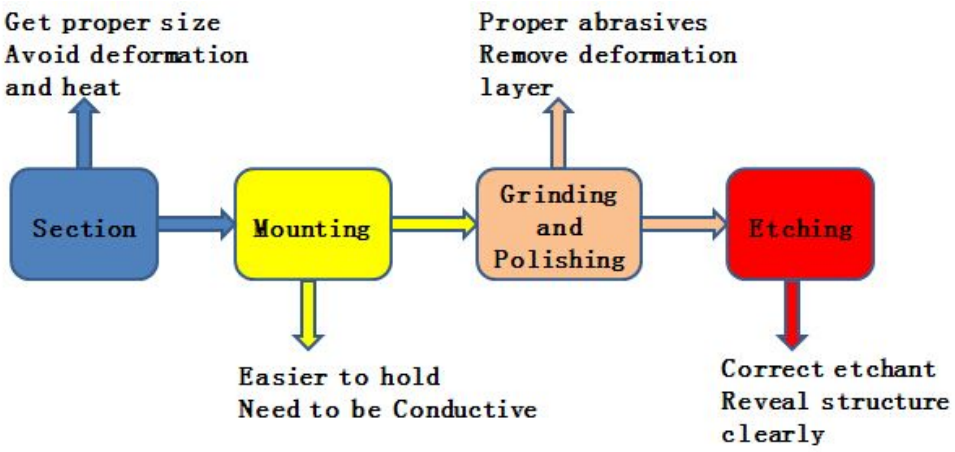

Figure 5. Summary of sample preparation procedure

4.2 PROCEDURES OF MICROSTRUCTURE ANALYSIS

4.2.1 Introduction

Microstructural analysis is an effective technique to indicate how heat treatments change the specific properties of the knife steels, since the properties changes will be reflected in the microstructures. To apply scientific analysis and get statistically-representative data, the procedures should be standardized to avoid noise factors during the experiment.

4.2.2 Procedures

4.2.2.1 Microstructure examination by optical microscope

Optical microscope is a reasonable technique for consistency examination. In this project, 500X is a proper magnification to get overall views of the microstructures of the samples.

Three test coupons in the same dimension, 1 inch X 4 inches, were heat treated for each group (austenizing/tempering combination). Each test coupon was

prepared using our standard procedures (detailed in Appendix 3). Next, three optical images were taken in different areas on each sample. The optical images of each group were compared to examine the consistency between different coupons and areas. The grain size, carbide distribution, and carbide fraction were checked to identify any significant difference between images. A consistent microstructure for different samples in each group was desired in the experiment.

After consistency examination, one sample was selected for SEM analysis. The selected sample should reveal clear microstructure and be etched properly to get high-quality images by SEM examination.

4.2.2.2 Microstructure examination by scanning electron microscope (SEM)

SEM is a stronger technique than optical microscopy to examine the microstructure, since it produces images with higher magnification and higher resolution. Images taken by SEM make it possible to observe the phase changes in detail and collect data accurately.

In the examination process, three magnifications, 1000X, 3300X and 10000X, were selected to observe the microstructures at different levels. The images taken at 1000X are better for an overall view and the images taken at 10000X are clear enough to observe characteristic structures of each grain, while 3300X images provide a balance between an overall view of the whole microstructure and high resolution.

To make sure the data from images are representative for statistical analysis, three images were taken in different areas under each magnification. The areas were selected randomly.

4.2.2.3 Data collection from SEM images

To a certain extent, the microstructure changes under different heat treatments can be visible to the naked eye. In this project, we also wanted to make a rigorous statistical analysis to indicate how the microstructure changes under different heat treatments. Therefore, every feature of the steel microstructure should be quantified and a large amount of data should be collected from the SEM images.

The size and location of each carbide grain are recorded in the data collecting process. From the raw data, we can get the average carbide size, carbides fraction, carbides count and interparticle spacing. The results from data collection help us to correlate the microstructures to mechanical properties and compare the different heat treatments.

4.3 PROCEDURES OF EDGED BLADE PERFORMANCE TESTS

4.3.1 Introduction

No matter how the heat treatment is applied or how the microstructure looks, the primary goal is achieving excellent mechanical properties for a knife blade. Therefore, a proper mechanical testing design will play an important role in this project.

Avoiding noise factors is the key point in the testing design. Many factors could be noisy in mechanical testing, such as operator, time, temperature and testing order. All factors were kept as consistent as possible in the mechanical testing. If there were factors that could not be controlled, a statistical method was applied to examine how these factors affect testing results.

Based on the mechanical properties we want to study, four tests are designed in this project.

Hardness: Rockwell Hardness C test (25 tests/heat treatment)

Toughness: 3-point bend test, Impact test (5 tests/heat treatment)

Edge retention: CATRA test (5 tests/heat treatment)

4.3.2 Procedures

4.3.2.1 Rockwell Hardness C Test

Hardness is the most common and fundamental mechanical test for steels. In this project, the Rockwell Hardness C test is applied, since it's easy to use, accurate and standard. The tester measures the hardness by measuring the resistance to penetration of an indenter [2]. There are also different scales that are determined by the indenter used and the load applied. The C scale is generally used in tool steel and stainless steel. A diamond with a cone angle of 120° and 150-kg load is used for C scale. The hardness number is given by Equation 1 **[**3**]**. Where, t is the indentation depth (*mm*).

$$HRC = 100 - 500t \quad \textbf{(1)}$$

The Rockwell Hardness tester used in this project is illustrated in Figure 6.

Figure 6. Rockwell hardness tester

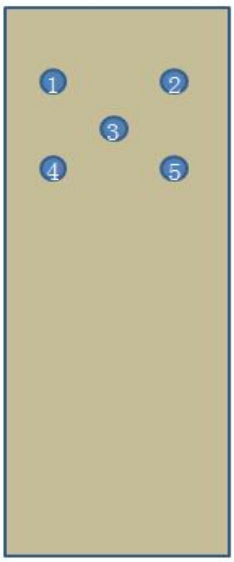

Figure 7. Five hardness readings

Five test samples with the same dimensions were tested for each group. Five readings were collected for each sample in different positions. The spacing of

these measure positions is compliant with ASTM E18-14a. The distance between the centers of two positions is larger than 3 times the diameter d ($1.5\,mm$) of the indenter, and the distance from the center of any position to an edge of the sample is larger than 2.5 times the diameter d of the indenter [18]. Also, the five testing positions are kept consistent in all samples (shown in Figure 7).

All tests were completed by two operators in one day. Both operator order and sample order were randomized. After data collection, a statistical method was used to examine whether the operator affected the testing results. There is no significant operator difference shown in the ANOVA table (see Table 18 in Appendix 4).

4.3.2.2 Impact test:

Toughness is a mechanical property that measures the ability of the material to resist fracture. An impact test is applied to measure this ability by measuring the energy absorbed during the fracture. Generally, a pendulum striker falls from a fixed height and the sample is fixed at the lowest point of the path. After breaking the sample, the striker goes back to a specific height that will be calculated and converted into the absorbed energy. Charpy U and V tests are widely used. The standard sample dimensions are the same in both Chapy U and V tests, however they require different shapes of notches.

When measuring smaller sample like knife blade material in this project, the Charpy U and V tests are not sensitive enough [3]. An alternative impact test was developed. The testing machine is shown in Figure 8.

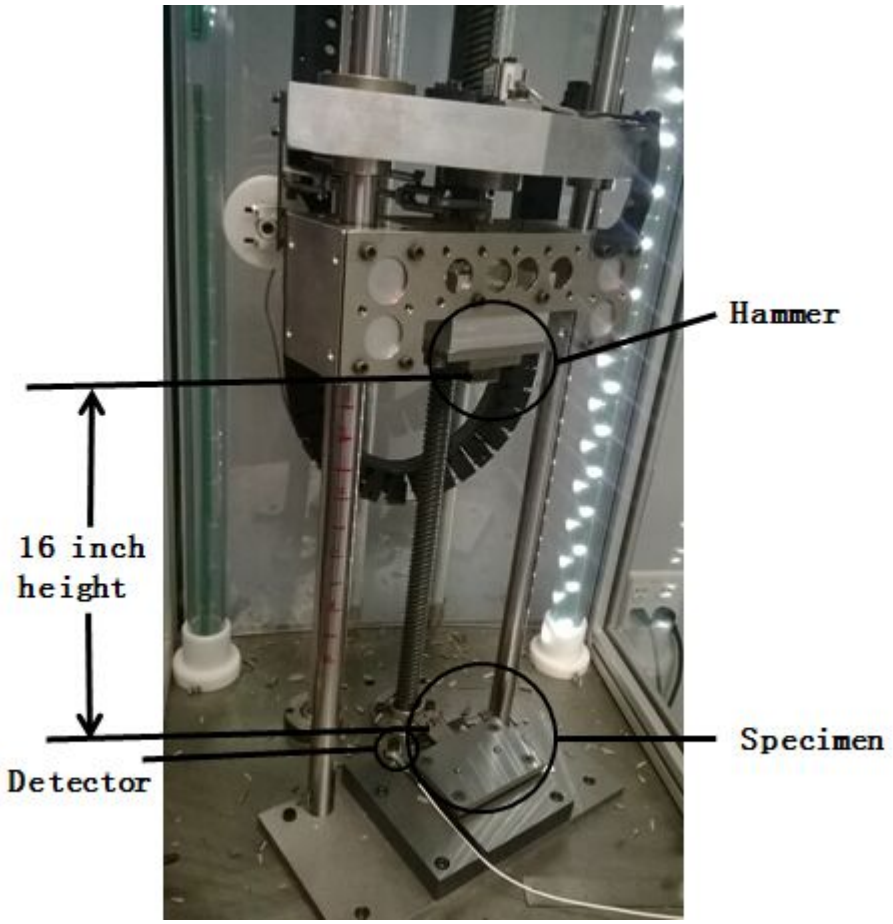

Figure 8. Impact test machine

As Figure 8 shows, a hammer with the weight of 11.5 lbs was set at a fixed height, 16 inch. The specimen was fixed at the bottom of the machine. Beside the specimen, a detector was placed to measure the impulse energy.

Temperature is also an important factor affecting the toughness performance. To avoid the noise from different temperatures, all of the impact tests were completed in one day.

For the first run of this test, there was no specimen fixed at the bottom. The hammer was dropped from a height of 16 inches. The impulse energy of free drop was measured. Then, five samples with the same dimensions for each group were tested in random order. The detector collected the impulse energy data. Finally, the absorbed energy was calculated as the difference between impulse energy of each run and the free drop energy.

4.3.2.3 3-Point bend test

The 3-Point bend test is a kind of failure strength test. A transverse force is applied on a sample until failure. In this type of test, the samples are usually rectangular in shape and the detailed dimensions are not standard. The test machine is illustrated in Figure 9.

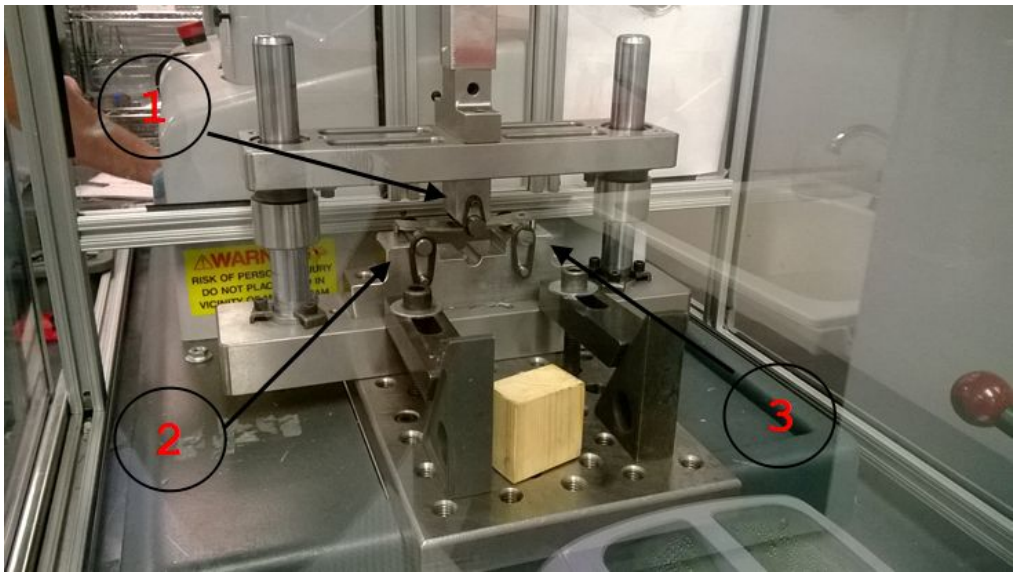

Figure 9. 3-Point Bend test machine

As Figure 9 shows, there are three contact points made by cylinders during the test. Point 1 contacts the middle of the specimen to provide a pressure load. Point 2 and Point 3 support the specimen at the ends. In the test, the load is

increased at a constant rate, the maximum load and the bend distance are recorded when the specimen fails.

In this project, five samples for each group were tested by the 3-Point bend test in a random order. Each of the samples was prepared in a standard size that had a thickness of 0.1 inch and a width of 0.7 inch. As for the test machine, it was also kept consistent during the test process. Therefore, all factors were fixed. The max load data is used to analyze the transverse failure performance.

4.3.2.4 CATRA test

High cutting edge stability is a characteristic performance of CPM-M4 steel. The CATRA test was developed to quantify this property. The CATRA test machine is shown in Figure 10.

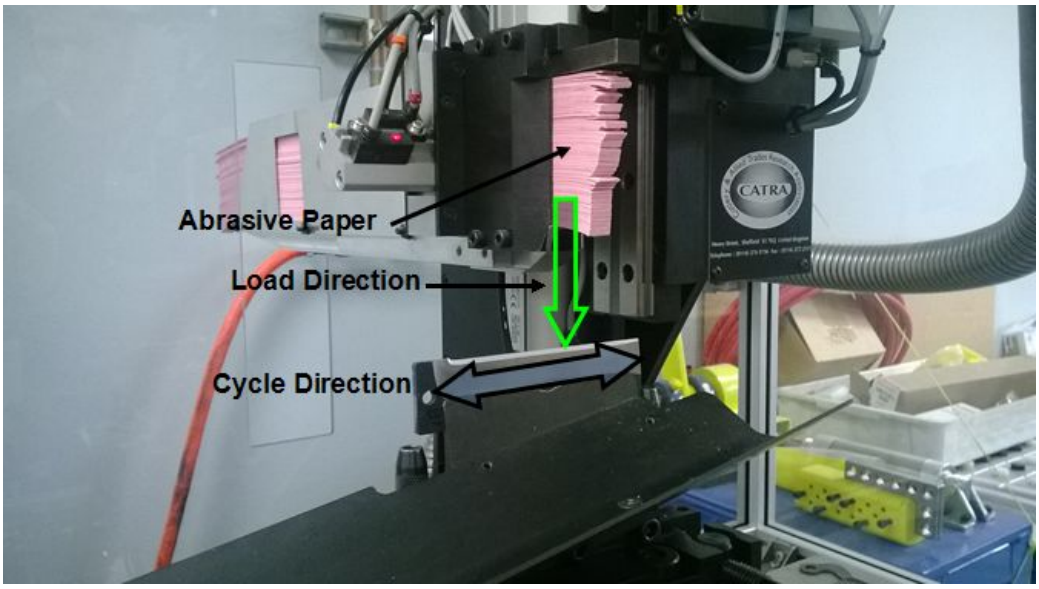

Figure 10. CATRA test machine

In the test, a fixed load was applied on the sharpened samples. The CATRA machine cycled the cutting edge a fixed distance horizontally. Abrasive paper was selected as the test media and the depth of cut for each cycle was measured to quantify the cutting property of samples. At least 20 cycles were repeated for each sample. If the final cut depth is larger than 10mm in the 20 cycles, the test would be repeated until the final cut depth is less than 10mm. To quantify the cutting properties of different samples, the sum of the first three cycles defines the initial cutting performance and the sum of first 20 cycles defines the cutting edge retention.

For consistency, all samples were prepared in a standard size and a standard sharpening process was applied on all samples. However, there are also many potential noise factors in the test. To avoid these factors, the test order was executed in five replications. There was one sample from each of the five heat treatments in each replication. For each replication, a same batch of abrasive paper was used and the tests were finished in one day. For the first three replications, the abrasive paper are from the same batch. A new batch of paper was used for the last two replications.

5 RESULTS

5.1 MICROSTRUCTURE:

In this study, although different heat treating parameters are used, the general microstructure of CPM-M4 steel is tempered-martensite with carbides of varying composition. As Figure 11 shows, the spherical carbides are distributed uniformly in the matrix. Due to the PM process, the carbide size is fine and uniform.

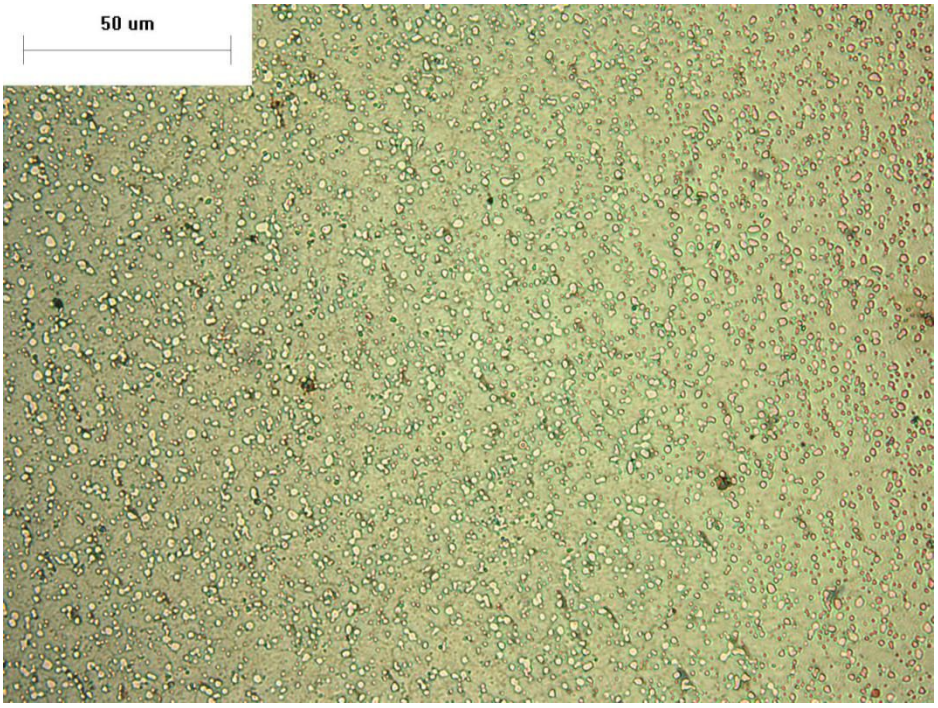

Figure 11. Optical microstructure of CPM-M4 steel, austenitized at 2100°F, tempered at 1025°F, magnification is 500X

Based on the element analysis results from the EDX analysis and the typical features of different phases, an SEM image with phase identification is shown in Figure 12. MC and M_6C are two major kinds of carbides distributed in the tempered-martensite matrix [16,17]. By EDX examination, the darker

MC carbides in the SEM image are vanadium-rich carbides. MC carbides usually appear spherical in shape and are distributed inside the matrix grains. On the other hand, the brighter M_6C carbides are molybdenum and tungsten-rich carbides. Molybdenum and tungsten contents are much higher than vanadium and chromium contents for these carbides. The EDX results are shown in Figure 13. In other steel alloy microstructures, vanadium carbides are usually small in size compared to other carbides. However, in this study, these two kinds of carbides do not show a large difference in their size. Powder metallurgy is the major reason for the lack of difference because it makes all of the carbides fine and uniform in size. As a result, the other carbides, such as the M_6C carbides, have a size similar to the vanadium-rich MC carbides.

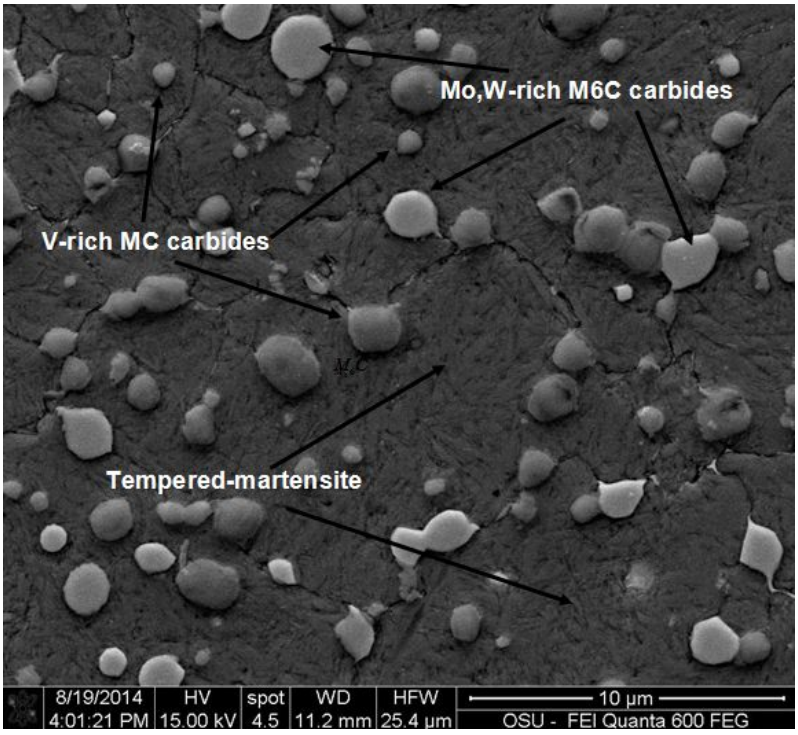

Figure 12. Phase identification of CPM-M4 steel, autenitized at 2200°F, tempered at 925°F

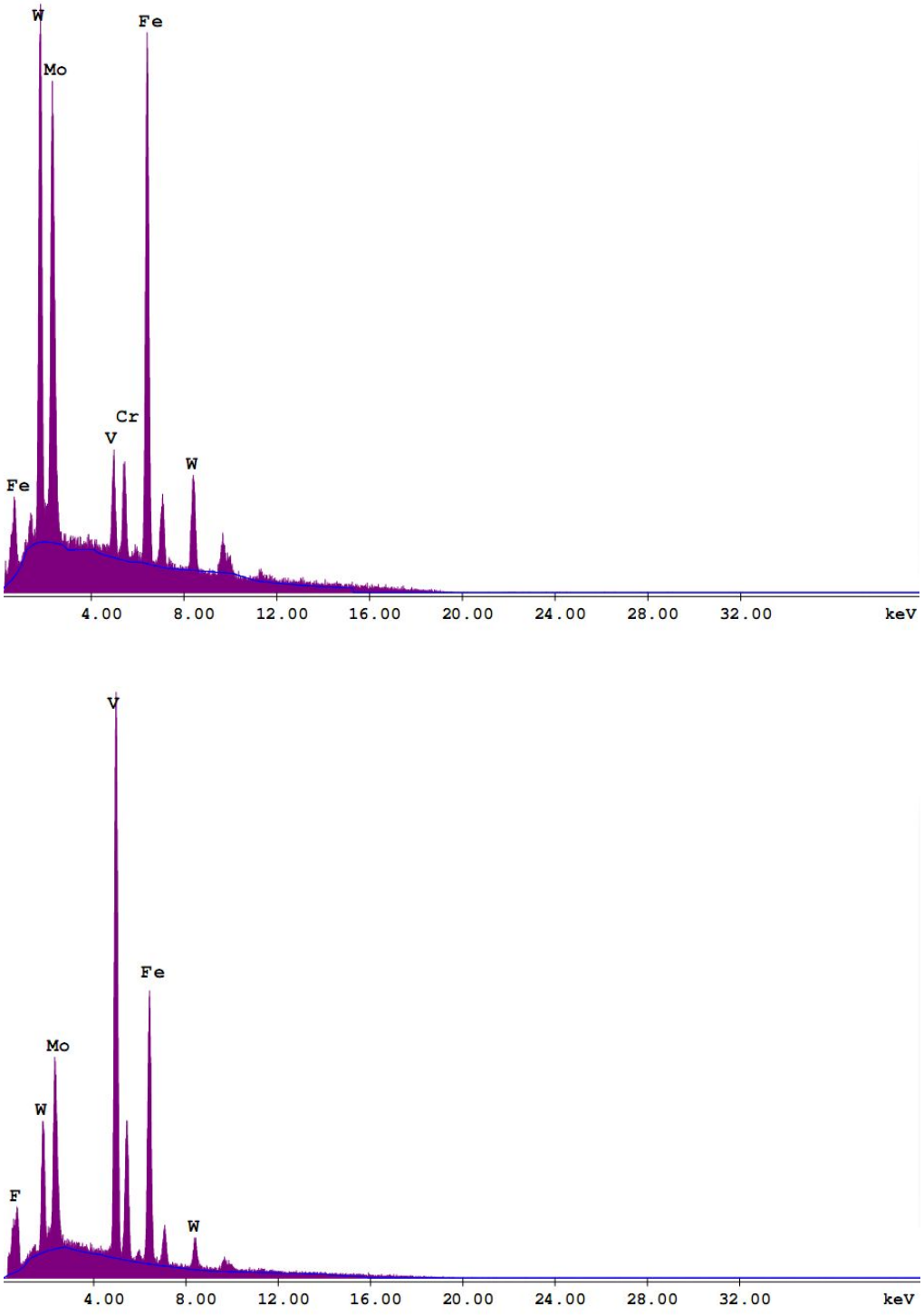

Figure 13. Chemical composition of the Mo,W-rich carbides (upper) and the V-rich carbides (below) from EDX analysis

Carbides fractions were calculated from the area fractions of three SEM images for each heat treatment group. Every carbide grain was traced to calculate their size. The results of the average carbide fraction and size

calculations are shown in Table 3 and Figure 14. SEM images of different heat treatment samples are shown in Figure 15.

Table 3. Average carbides fraction and size of different heat treatments

	A-T-	A-T+	Center	A+T-	A+T+
Carbides Fraction (%)	17.44	17.31	19.62	14.71	14.15
Standard Deviation	1.39	1.12	2.50	0.90	0.82
Carbides Size (μm^2)	0.86	0.93	1.17	0.89	1.06
Standard Deviation	0.91	1.00	1.16	0.99	1.02

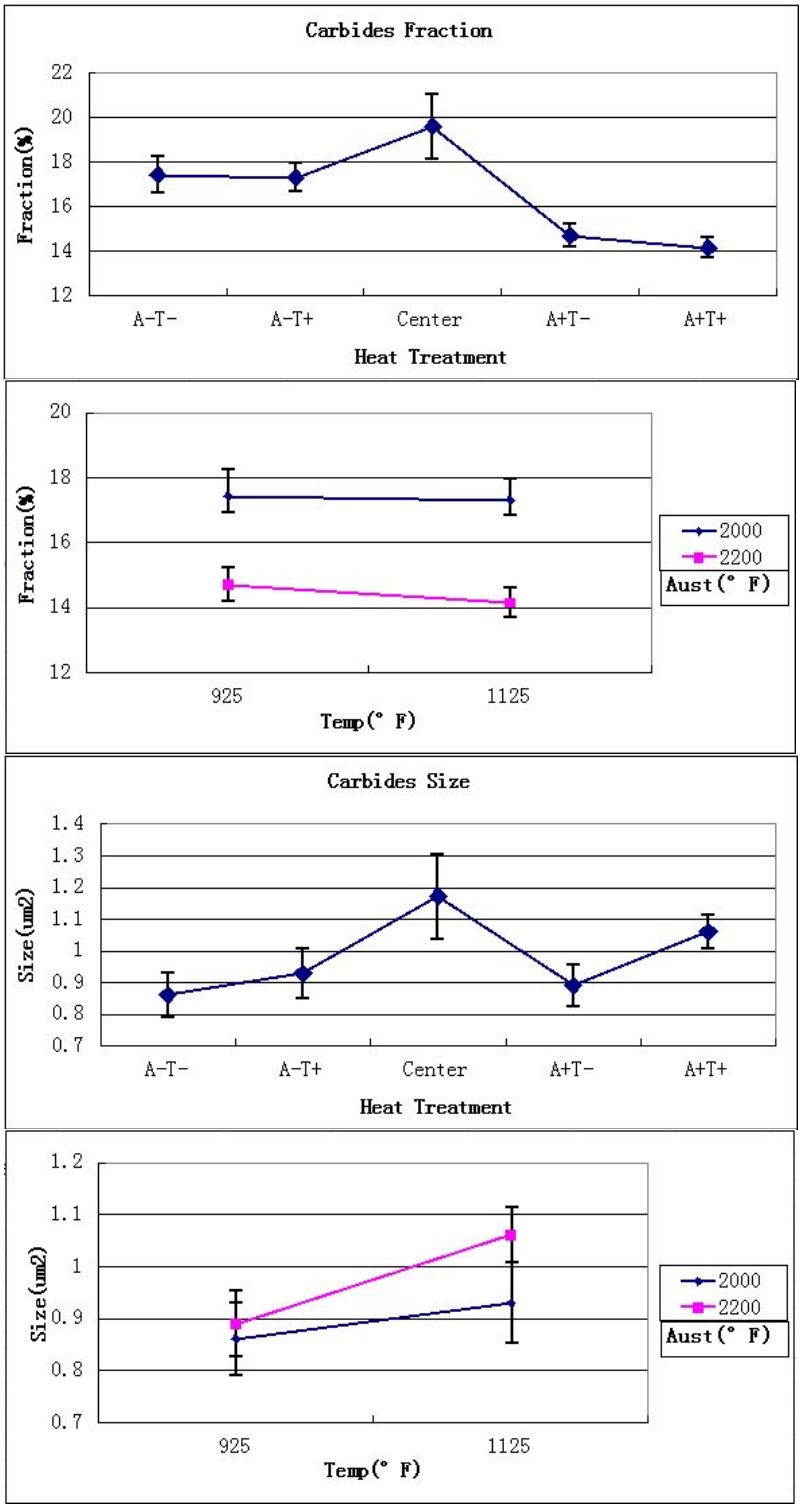

Figure 14. Comparison of carbides fraction and size among heat treatments

The center heat treatment (austenitized at 2100°F, tempered at 1025°F) gives the highest values for both carbides fraction and size compared to the four

other heat treatments. The center treatment has a carbide fraction of 19.62% and an average size of 1.17 μm^2 . From the ANOVA (analysis of variance) table (see Table 11 in Appendix 4), the carbides fractions show a significant difference between samples under different austenitizing temperatures. A lower austenitizing temperature (2000°F) gives 17.44% and 17.31% carbides fractions while a higher austenitizing temperature (2200°F) give 14.71% and 14.15% carbides fractions. However, with a constant austenitizing temperature, similar carbides fractions are obtained for different tempering temperatures. As for carbides size, lower austenitizing temperatures give an average carbides size of 0.86 μm^2 and 0.93 μm^2 while a higher austenitizing temperature gives an average carbides size of 0.89 μm^2 and 1.06 μm^2 . Under the same austenitizing temperature, carbides sizes increase with increasing tempering temperatures. On the other hand, the average carbides size also show a significant difference between different austenitizing temperatures (see Table 10 in Appendix 4), especially with the center austenitizing temperature (2100°F).

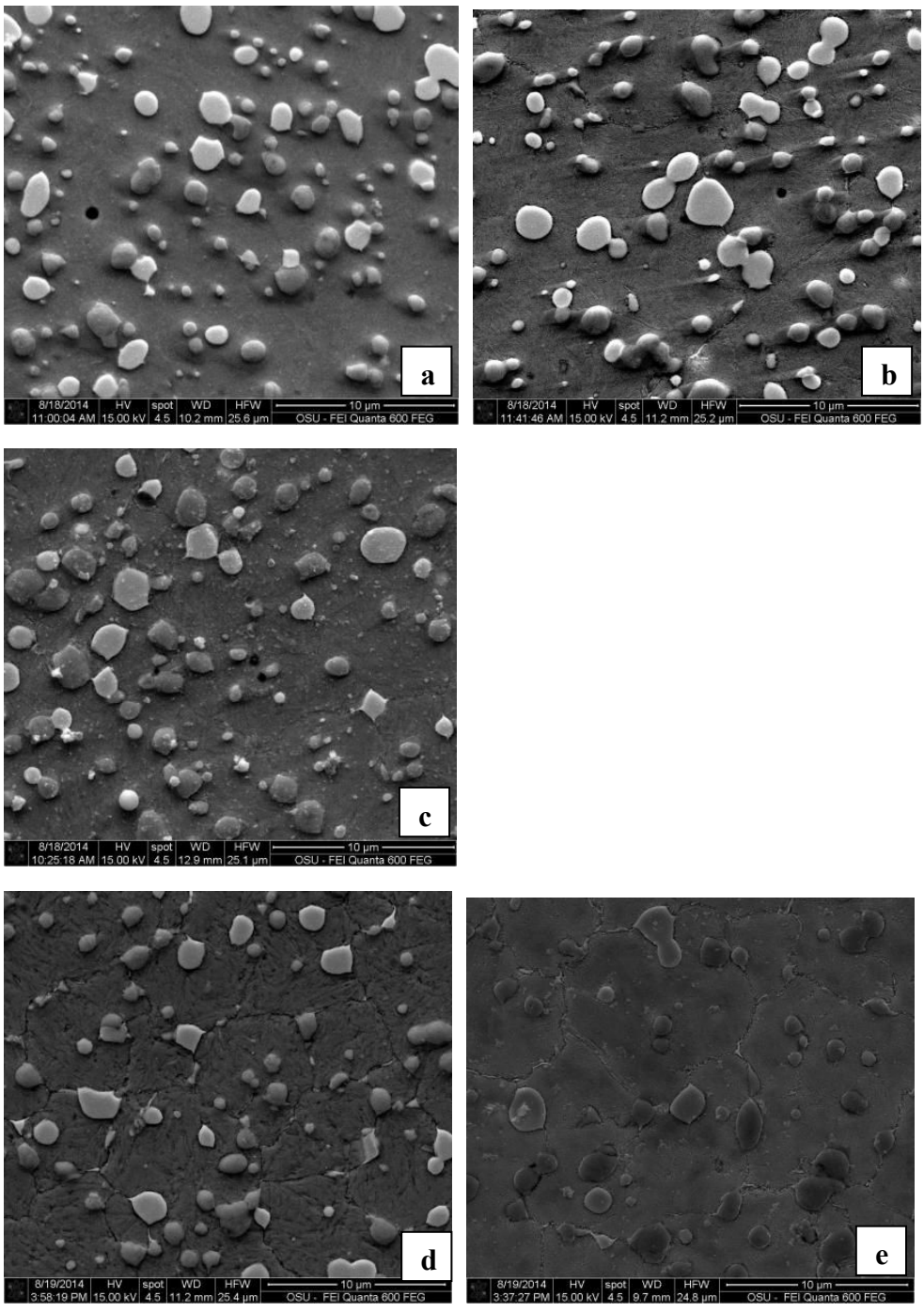

Figure 15. SEM images of different heat treatment samples (a-e represent A-T-, A-T+, Center, A+T-, A+T+, respectively)

The results of carbides count and interparticle spacing are shown in Table 4. The carbides count results were calculated from the average of three observations. Since the total area of each image is fixed in the microstructure analysis, the carbides count can be seen as a measurement of carbide density.

In Figure 16, the A-T- heat treatment gives highest value of carbides count. Both austenitizing temperature and tempering temperature have significant effects (see Table 12 in Appendix 4). The carbides count decreases with increasing austenitizing and tempering temperatures. The results of carbides count range from 65 to 106.

The distance from each carbide to the nearest carbide is identified as the interparticle spacing. The results were calculated from the average of all carbides in each SEM image. There are more than 200 carbides that were measured, therefore the standard error is very small in this measurement. As shown in Figure 16, the A+T+ heat treatment shows the highest value which is 1.25 μm . Both austenitizing temperature and tempering temperature have significant effects (see Table 13 in Appendix 4). The interparticle spacing increases with increasing austenitizing and tempering temperatures.

Table 4. Carbides count and interparticle spacing for different heat treatments

	A-T-	A-T+	Center	A+T-	A+T+
Carbides Count	106.0	95.0	84.0	85.0	65.0
Standard Deviation	9.54	9.00	12.53	9.61	7.51
Interparticle Spacing (μm)	0.92	1.01	0.99	1.08	1.25
Standard Deviation	0.43	0.48	0.51	0.46	0.53

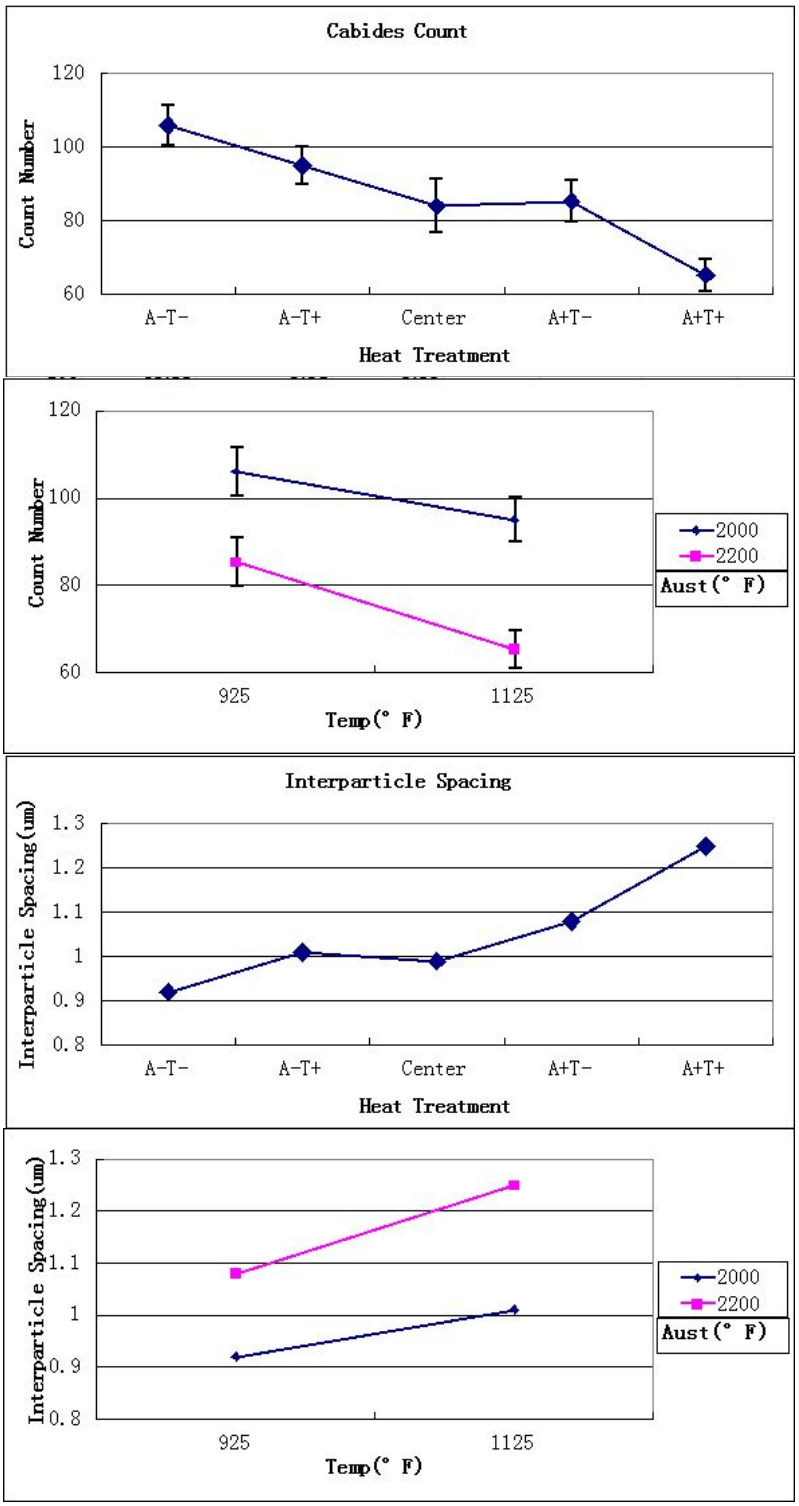

Figure 16. Comparison of carbides count and interparticle spacing among different heat treatments

5.2 EDGE PERFORMANCE

5.2.1 Hardness Test

By controlling heat treatment parameters, values from 57.72 HRC to 66.58 HRC were observed for the hardness, which are shown in Table 5. Five samples were tested for each heat treatment and five points were measured for each sample. Data in Table 5 are the average and the standard deviation of the 25 measurements for each heat treatment.

Table 5. Hardness results of different heat treatment samples

	A-T-	A-T+	Current	A+T-	A+T+
Hardness (HRC)	63.5	57.7	63.9	66.6	60.8
Standard Deviation	0.52	0.46	0.41	0.43	0.45

For lower austenitizing temperature, measured hardness decreased from 63.5 HRC to 57.7 HRC by increasing the tempering temperature, while increasing tempering temperature decreased the measured hardness from 66.6 HRC to 60.8 HRC for higher austenitizing temperature. A moderate hardness, 63.9 HRC, was obtained for the current heat treatment. From the ANOVA table (see Table 14 in Appendix 4), both parameters can change the hardness results significantly. Higher austenitizing temperature and lower tempering temperature give higher hardness values. A comparison is shown in Figure 17. The error bars (representing standard error in all figures) in the figure are too small to be visible.

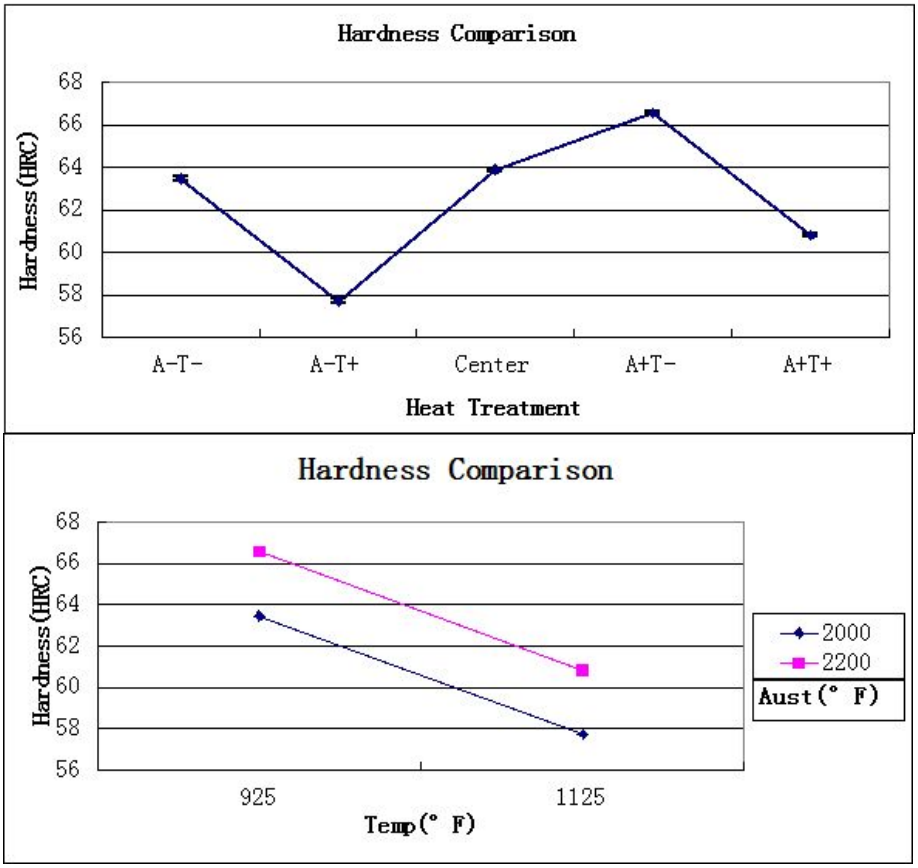

Figure 17. Comparison of hardness among different heat treatments

5.2.2 3-Point Bend test

In the 3-Point bend test, all specimens were made with the same dimensions and maximum loads were recorded when the specimen failure occurred. Five tests were done for each heat treatment sample. The value of the maximum loads were measured for five tests for each heat treatment. The average and the standard deviation of the five measurements are shown in Table 6.

Table 6. 3-Point Bend results for different heat treatment samples

	A-T-	A-T+	Center	A+T-	A+T+
Max Load (lbs)	894.8	872.4	971.5	805.8	830.6
Standard Deviation	15.2	16.6	19.5	52.3	71.8

Obviously, higher result values for the 3-Point bend test correspond to higher failure strength that is a desired property for knife blade materials. The center heat treatment gives the highest value result, which is 971.5 lbs. The other four heat treatments obtain the max load ranging from 805.8 lbs to 894.8 lbs. Lower austenitizing temperature gives a higher value compared to higher austenitizing temperature. As for tempering temperature, it doesn't have a significant effect on the test results (see Table 15 in Appendix 4). A comparison of the maximum load between different heat treatments is shown in Figure 18.

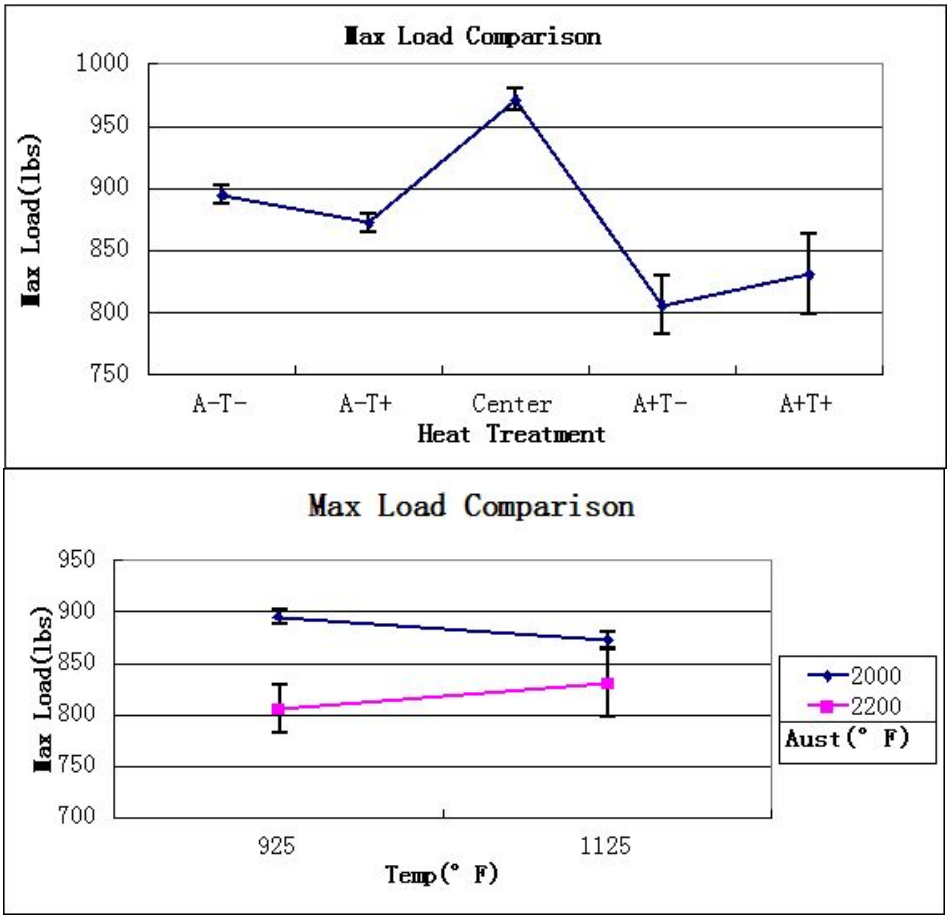

Figure 18. Max load in 3-Point Bend test comparison among different heat treatments

5.2.3 Impact test

Since this is a destructive test, five specimens were prepared for each heat treatment. First, the free drop energy in the no-sample loading condition was measured, which was 15.333 ft*lbs. Then tests were run for each specimen and the detector measured the impulse energy in the sample loading condition. The equation below gives the energy absorbed by the specimens:

Absorbed energy = Free drop energy - Impulse energy with sample loading **(2)**

The average value and standard deviation of absorbed energies were used as the impact test result and are shown in Table 7.

Table 7. Impact test results for different heat treatment samples

	A-T-	A-T+	Center	A+T-	A+T+
Energy Absorbed (ft*lbs)	11.47	11.34	8.80	8.48	7.89
Standard Deviation	0.93	1.50	1.07	1.39	1.15

From the results, samples austenitized at the lower temperature absorbed more energy than both the center heat treatment samples and the higher austenitized samples. About 11 ft*lbs of energy was absorbed by the samples with lower austenitizing temperature. The center heat treatment does not perform as well in the impact test, absorbing only 8.8 ft*lbs of energy in the failure. The other two heat treatments, austenitized at a higher temperature, gave impact results of 8.48 ft*lbs and 7.89 ft*lbs. The tempering temperature does not affect the impact results significantly (see Table 16 in Appendix 4), creating only a small change. The comparison is shown in Figure 19.

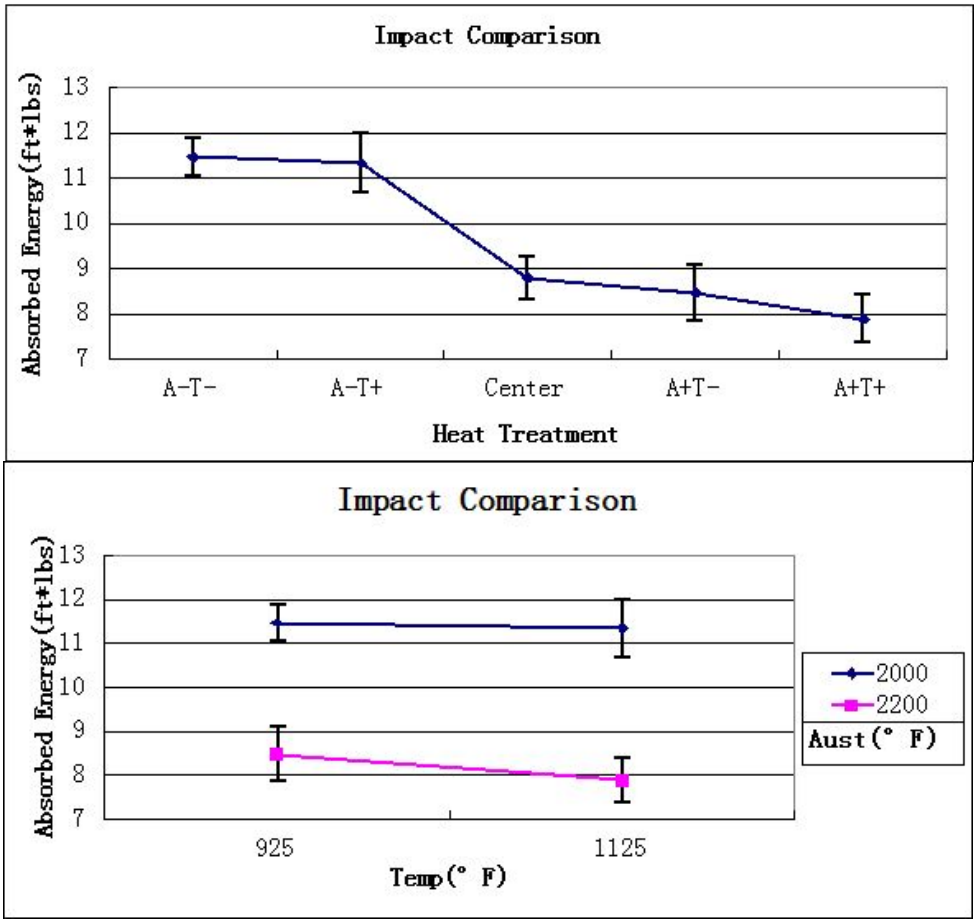

Figure 19. Impact results comparison among different heat treatments

5.2.4 CATRA test

In the CATRA test, samples were arranged into five replications. The test results are shown in Table 8 and Figure 20. Both initial cutting performance and cutting edge retention results are calculated from the average values of responding replications in Figure 20, while the results in Table 8 are calculated from the average values of all of the five replications.

Table 8. CATRA test results for different heat treatment samples

	A-T-	A-T+	Center	A+T-	A+T+
Initial Cutting Performance (mm)	107.7	98.0	104.3	113.6	97.1
Standard Deviation	11.0	14.9	10.7	16.8	9.6
Cutting Edge Retention (mm)	399.3	370.8	400.6	439.5	365.2
Standard Deviation	42.1	56.5	50.7	78.8	44.0

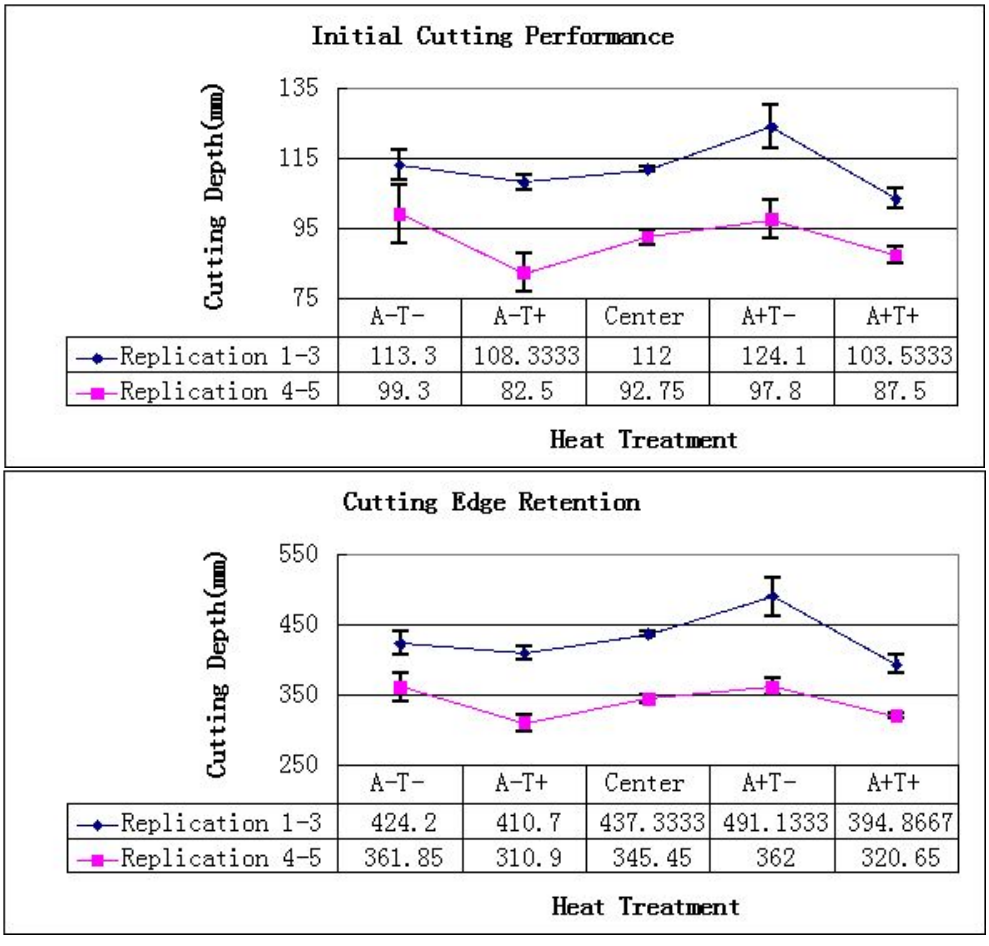

Figure 20. CATRA test results for different heat treatments

Figure 20 shows that the test results of replication 4 and 5 are much lower than the first three replications due to the different batch of abrasive paper. However, the different batch of paper does not change the trend among the heat treatments. Moreover, comparing the two measured performance in CATRA test, the initial cutting performance and the cutting edge retention have the same trend among different heat treatments. The A+T- sample provides the highest values for both performances. As shown in Figure 21, lower tempering temperature provides better performance than higher temperature. As for austenitizing temperature, there is not a clear effect on performance. When tempered at a lower temperature, the higher austenitizing temperature achieves higher values in cutting performance. If the tempering temperature is higher, the effect of austenitizing temperature becomes indistinct. The center heat treatment gives medium values in the CATRA test.

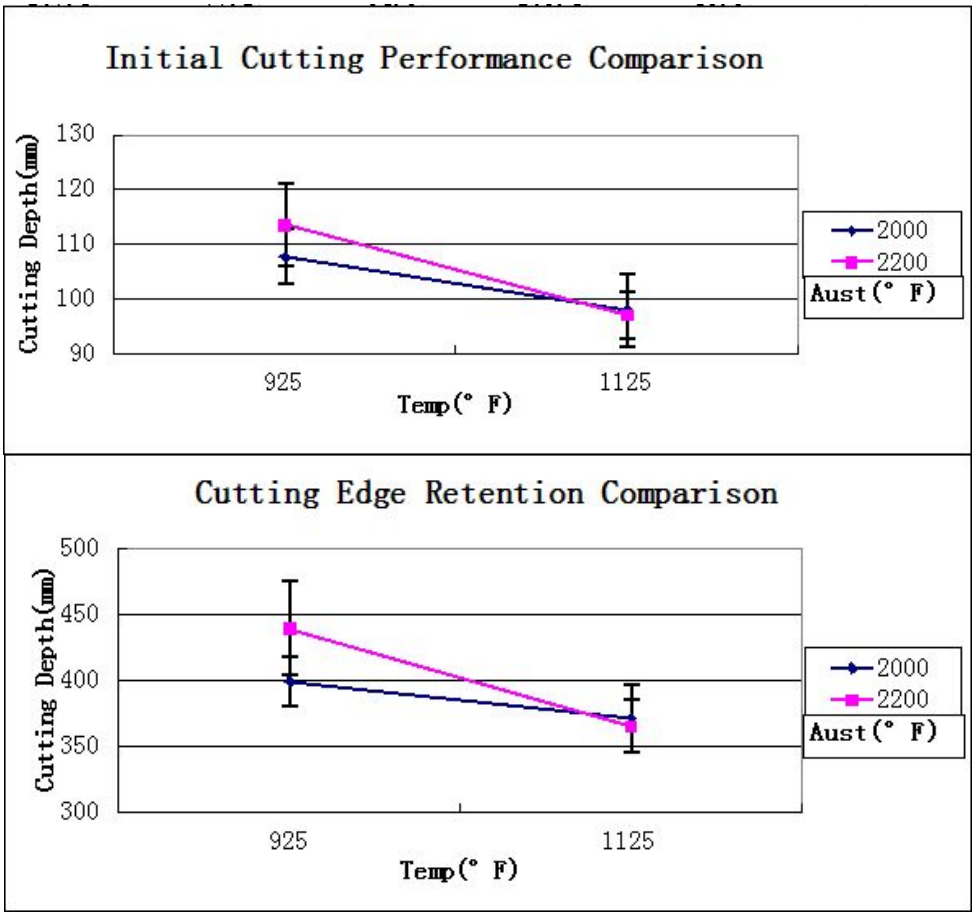

Figure 21. CATRA results comparison among different heat treatments

5.3 SUMMARY OF RESULTS

The results of all edge blade performance tests and microstructural analysis are summarized in Table 9. The data are average values of all measurements for different tests.

Table 9. Summary of edge performance test results and microstructure analysis

	A-T-	A-T+	Center	A+T-	A+T+
Carbides Fraction (%)	17.44	17.31	19.62	14.71	14.15
Carbides Size (μm^2)	0.86	0.93	1.17	0.89	1.06
Carbides Count	106.0	95.0	84.0	85.0	65.0
Interparticle Spacing (μm)	0.92	1.01	0.99	1.08	1.25
Hardness (HRC)	63.5	57.7	63.9	66.6	60.8
3-Point Bend (lbs)	894.8	872.4	971.5	805.8	830.6
Impact (ft*lbs)	11.47	11.34	8.80	8.48	7.89
Edge Retention (mm)	399.3	370.8	400.6	439.5	365.2

6 DISCUSSION

From the previous chapters, we can see that different heat treatments lead to a significant difference in both microstructure and edge blade performance. Based on the experimental results and basic principles in metallurgy, the characteristic performance can be correlated to the specific heat treatment parameters and their microstructures.

Table 4 and Figure 14 suggest that the austenitizing temperature is the only parameter determining the carbides fraction. The highest carbides fraction is achieved by the center heat treatment that is a medium austenitizing temperature (2100°F). In the austenitizing process, carbon atoms and alloy elements atoms in carbides dissolve into the austenite matrix, however, in different ways. Carbon dissolves as interstitial atoms, while alloy elements can only dissolve in the matrix by substituting the iron atoms. The diffusion coefficient of carbon and alloy elements can be defined as the equation below:

$$D = D_0 \exp(-\frac{Q_d}{RT}) \quad \textbf{(3)}$$

where, D is the diffusion coefficient, D_0 is the material constant, Q_d is the activation energy, R is gas constant and T is temperature.

According to Equation 3, higher austenitizing temperature will accelerate the dissolving process for both carbon and alloy elements. Complete carbide dissolution in the austenitizing process can promote carbides precipitation in both the quenching and tempering processes, because more carbon dissolving in a matrix can create more distortion and lead to more defects during the

quenching process. The high internal stress caused by the distortion of the lattice structure will provide the driving force for carbides precipitation [19]. Moreover, complete carbide dissolution can also achieve a more uniform carbon distribution, which means carbon atoms have more opportunities to form carbides with the alloy elements. Compared to interstitial atoms, substitutional atoms have much lower mobility in the carbide precipitation process, which means that more alloy elements dissolved in the matrix will make it harder to re-form carbides with carbon atoms. Additionally, the excessive dissolving of alloy element will change the lattice structure and a possible release of internal stress will decrease the driving force for carbides precipitation. Based on these facts, the carbon dissolving and alloy substitution processes should be balanced to maximize the carbides fraction. When austenitizing at relatively low temperatures, the undissolved alloy elements are enough to form carbides with carbon atoms, carbides formation process will be promoted by the increasing driving force with austenitizing temperature. However, when the austenitizing temperature is relatively high, excessive alloy elements dissolved in the matrix will limit the carbides fraction in the final microstructure. Also, the carbon dissolving process can be saturated at a higher austenitizing temperature, which means it would not promote carbides formation any more. The lower driving force caused by excessive alloy element dissolving will lead to a lower carbides fraction. The experimental results also verify that increasing the austenitizing temperature does not have a monotonous effect. A balance point can be obtained by controlling the

austenitizing temperature, if a higher carbides fraction is desired for the final microstructure.

The experimental results show that tempering temperature does not affect the carbides fraction significantly. However, the fact that average carbide size is affected by the tempering temperature confirms the process of carbon diffusion during tempering. Carbides grains grow from the diffusion process. A higher tempering temperature corresponds to a larger carbides size. To observe the effect of the carbides nucleation process during tempering, an as-quenched sample needed to be analyzed. The carbides fraction of an as-quenched sample is 17.53% under the center austenitizing temperature (2100°F). The carbides fraction observed is lower than the 19.62% observed from a corresponding tempered sample. This demonstrates that there exists carbides growth or nucleation during tempering, however most of carbides form before the tempering process. Comparing the average size of carbides in as-quenched and tempered samples, the carbides growth is not very clear (see Table 17 in Appendix 4). Tempering only increases the carbides size from $1.123\,um^2$ to $1.172\,um^2$. That means that the carbides nucleation exists during the tempering and will increase the carbides fraction. From these results, we can see that the nucleation process is not influenced by the tempering temperature used. Since a double tempering process is developed to achieve full carbides precipitation for CPM-M4 steel, the carbides fraction will not be changed by different tempering temperature. Additionally, the selected tempering temperature should be relatively high to achieve secondary hardening. In this experiment, the lower tempering temperature, 925°F, is still

high enough to get a nearly complete carbide nucleation. Both long time and high temperature make it easier to form a complete carbides nucleation.

Moreover, carbides are an important phase in steels. Because of their higher hardness and the specific properties relating to their alloy elements, a higher volume of carbides is usually desired to increase the overall properties for knife blades, especially for wear-resistance [2]. In this study, carbides fraction shows a clear relationship with the max load observed in the 3-Point bend test. As a failure strength measurement, a high value of the max load in 3-Point bend test is desirable for knife blade materials. From Figure 22, we can see that the carbides fraction has a strong correlation with the max load in 3-Point bend test. The highest carbides fraction achieves the maximum max load. Meanwhile, if we are just concerned about the alternative heat treatments, only austenitizing temperature has significant effects. Different tempering temperatures only produce a small change in the max load observed in the 3-Point bend test, as seen in Figure 18. Also, hardness results do not show a clear relationship with 3-Point bend results. Higher tempering temperature leads to a significant drop in hardness. However it does not affect the max load in the 3-Point bend test significantly. Based on these facts, we can see that the carbides fraction is highly correlated to the max load in the 3-Point bend test, even if the fraction of carbides phase is much smaller than that of the matrix. The reason for this is that the failure strength depends more on the hardest phase, and the hardness of carbides phase is much higher than that of the matrix. In particular, for CPM-M4 steel, VC carbides, the most common type of carbides in CPM-M4 steel, are almost the hardest known carbides [2].

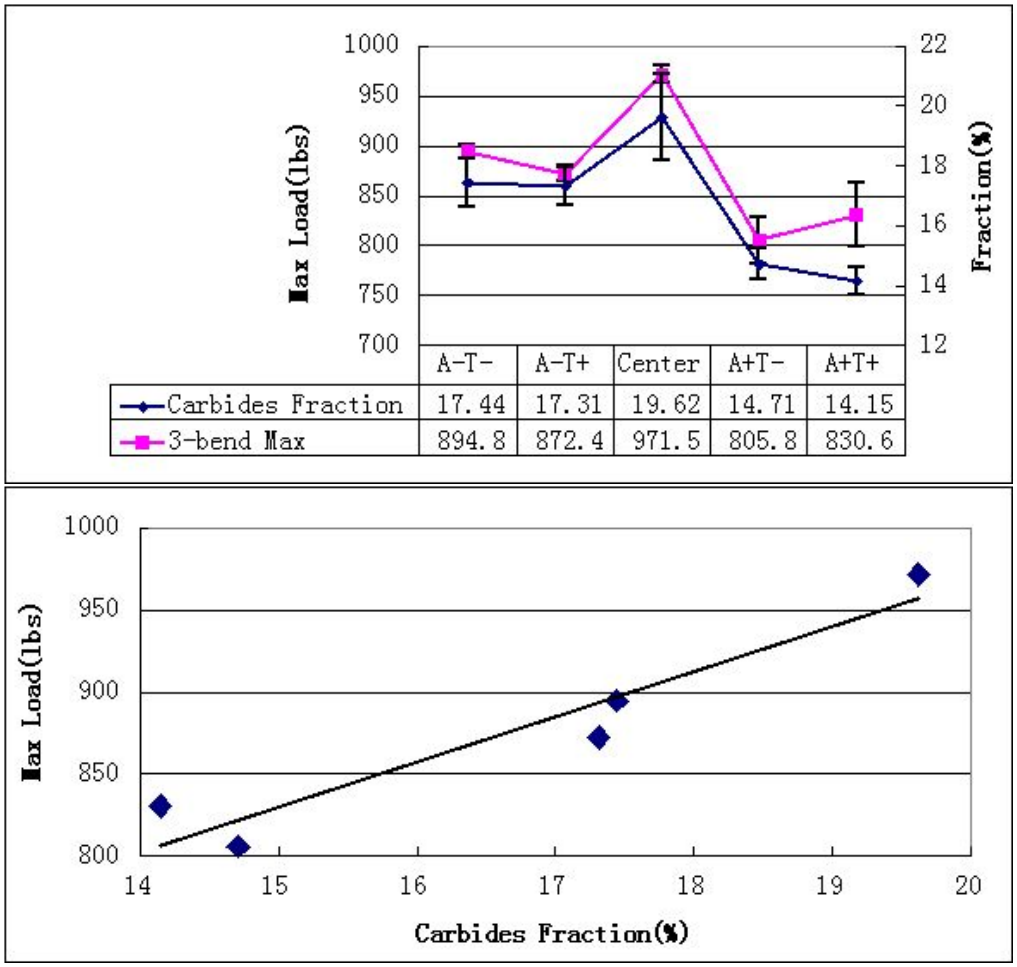

Figure 22. Comparison of carbides fraction and max load in 3-Point bend test for different heat treatments

Hardness depends more on the matrix. Both austenitizing and tempering temperature have significant effects on hardness, although in different manners. Higher austenitizing temperature will accelerate the dissolving of the alloy elements from carbides, leading to a harder matrix through solid solution strengthening. In the tempering process, higher temperature will promote the tempered-martensite transformation in the as-quenched structure, causing hardness to drop significantly. As Figure 23 shows, the hardness results have no clear relationship with the carbides fraction or size, which also

confirms that the softening of martensite matrix will determine the hardness of the final product.

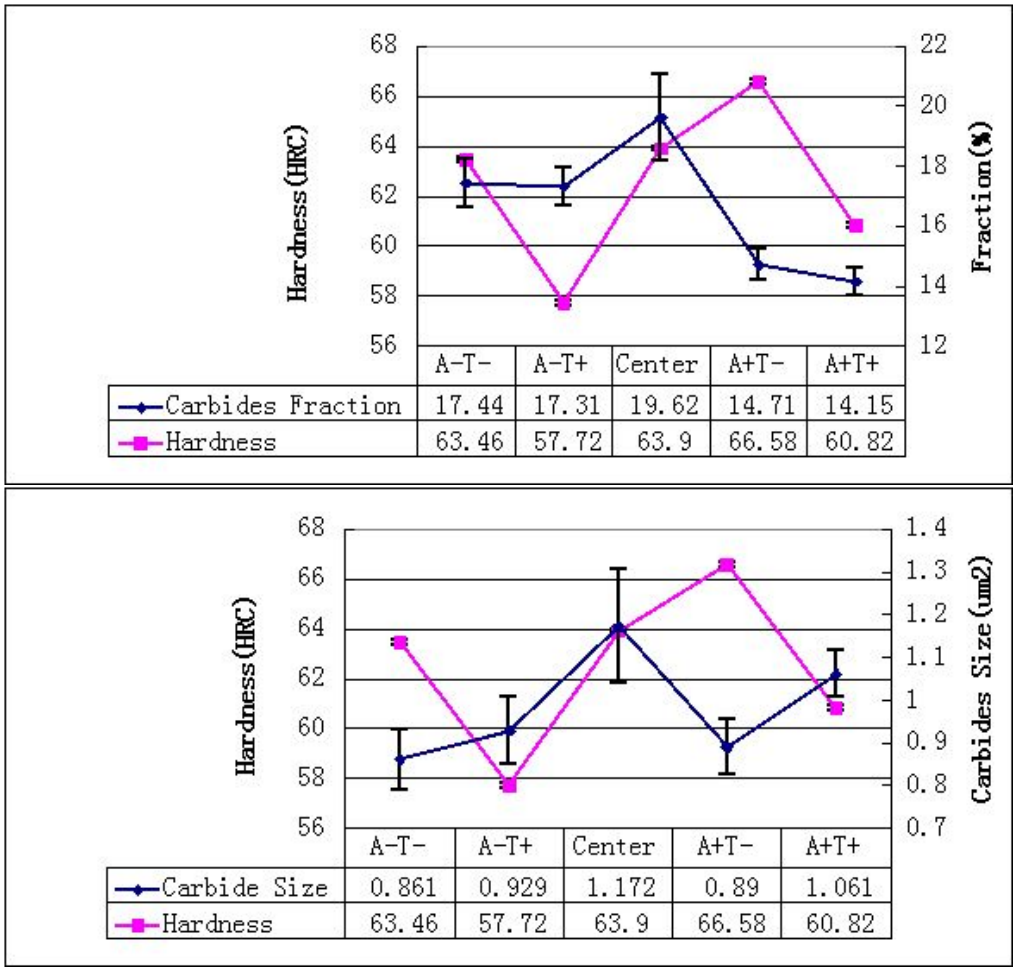

Figure 23. Comparison of hardness results with carbides fraction and carbides size

As for the impact test, the results are unexpected. The austenitizing temperature is the only significant factor affecting the absorbed energy observed. Under the same austenitizing temperature, tempering doesn't change the impact toughness significantly. Even when a higher tempering temperature was applied, the impact toughness dropped slightly, and the corresponding hardness dropped significantly. In Figure 24(b), the impact toughness

decreases with increasing austenitizing temperature. This means that more dissolved alloy elements in the matrix can lower the impact toughness. The reason for this is that the solid solution strengthening by dissolving alloy elements leads to a decrease in the toughness of the materials [20]. However, the matrix is not the only reason in this case. We can see that the impact toughness of the current heat treatment is lower than the trend line in Figure 24(b). The highest carbides fraction of the current heat treatment is responsible for this divergence. The reason behind this is that carbides usually perform as ceramic materials when the failure happens. Although carbides make it harder to break the material, it also coincides with a lower ductility. Therefore, an accelerated decrease on the impact toughness occurred in the center heat treatment.

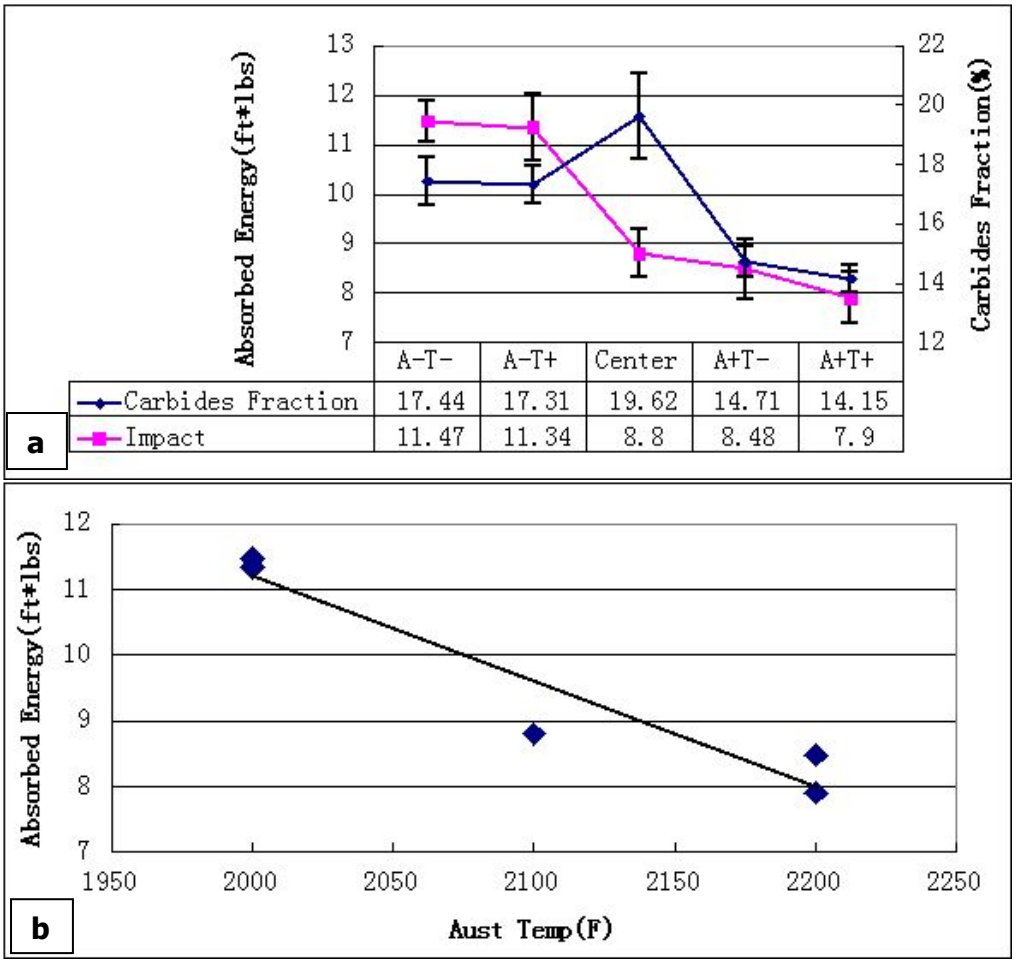

Figure 24. Comparison of impact toughness with austenitizing temperature and carbides fraction

Additionally, a higher absorbed energy observed in the impact test responds to a higher carbides count as Figure 25 shown. When a stress is applied on the material, the dislocations in the crystal structures can move allowing for distortion. However, the carbides can act as the pinning points to restrain the movement of the dislocations. This means that more energy is needed to break the material, if there are more carbides existing in the material.

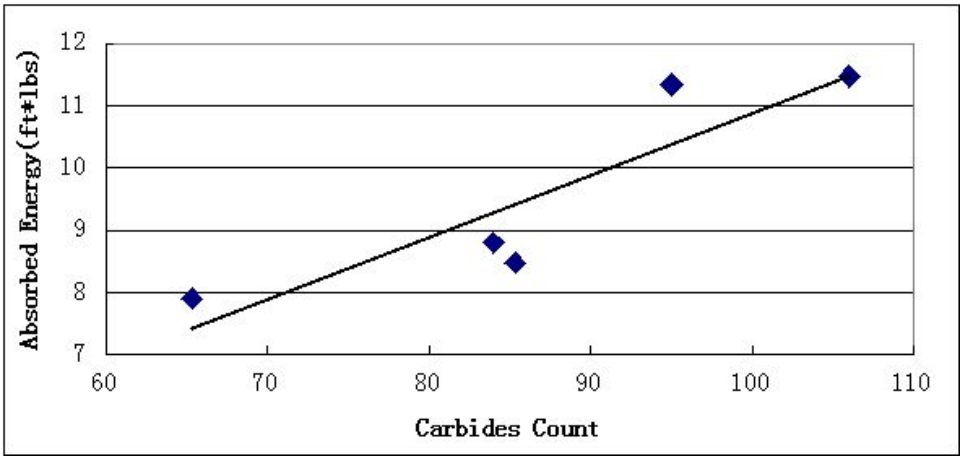

Figure 25. Comparison of impact test results with carbides count

Then, comparing to the hardness results in Figure 17, although lower austenitizing temperature provides a relative lower hardness, tempering temperature can be lowered to increase the hardness without decreasing the impact toughness. This should be a better heat treatment for balancing hardness and toughness rather than just controlling the tempering temperature.

According to the results from the CATRA test, improved cutting edge retention is accompanied with the higher initial cutting performance. The A+T- sample gives the highest values in both two measurements. In most of previous studies, the wear performance is attributed to the carbides contents. Larger carbides fraction and harder carbides phase usually provide better wear performance [16,17]. However, in this study, no clear relationship was identified between the edge retention performance and the carbides phase. In Figure 26, we can see the edge retention performance decreases significantly when the tempering temperature is increased. However, under the same austenitizing temperature, the carbides fraction does not show a significant change with different tempering temperature. As for the center heat treatment,

the edge retention performance is not the best, although it provides the highest value of carbides fraction. Similarly, there is no clear relationships between edge retention and other measurements of carbides phase, such as carbide size, count and interparticle spacing. This case is also same for the initial cutting performance.

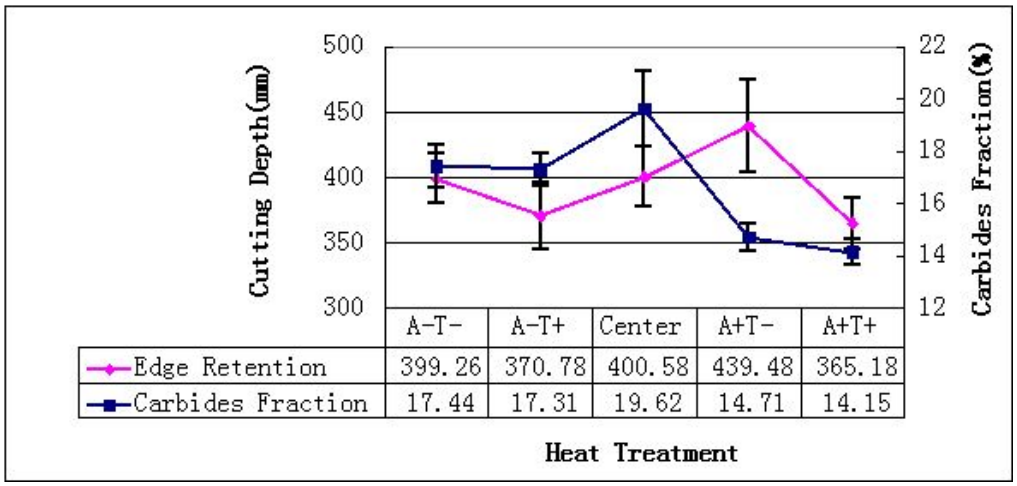

Figure 26. Comparison of cutting edge retention results with carbides fraction

After comparing to other edge blade performance measurements, the edge retention performance only relates to the hardness results. In Figure 27, the edge retention performance is increased with increasing hardness. The A-T- and the center heat treatment (marked in red circle in Figure 27) achieve similar edge retention performance and have similar hardness values. However, the carbides fraction of the center heat treatment is 19.62% compared to 17.44% in A-T- heat treatment. Therefore, we can conclude that the hardness of material is highly correlated to the edge retention test rather than the carbides phase. The major reason for the disagreement with previous studies is that the edge retention test we used is not a rigorous wear-resistance test.

When testing all samples were sharpened in a standard process and the total cutting depth defines the edge retention performance rather than the mass loss during the test. The measured performance is not only the wear-resistance of the materials, the retention of the sharp angle of knife blade also contributes to the edge retention performance. Although the harder carbides phase can make the material more abrasive, a higher general hardness provides better retention performance for the blade edge sharpness.

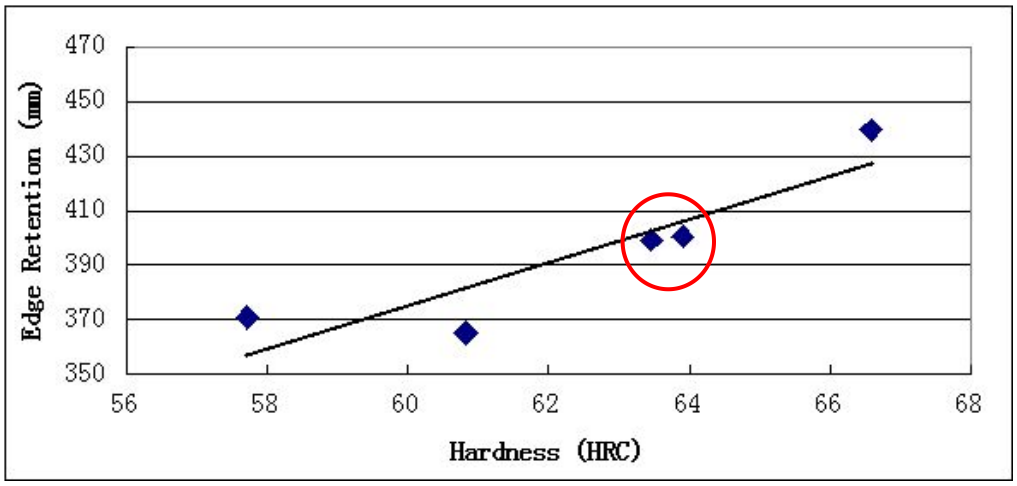

Figure 27. Comparison of cutting edge retention results and hardness

7 CONCLUSION

The effects of heat treatment for CPM-M4 steel have been studied in this thesis. In the experiment, five different heat treatments were applied by controlling the austenitizing temperature and tempering temperature in the heat treatment process. Four tests were used to evaluate the edge blade performance with respect to different heat treatment parameters. The four tests were hardness test, 3-Point bend test, impact test and CATRA test. Additionally, the microstructures of the CPM-M4 samples were analyzed to correlate their characteristic properties and microstructures to better understand how to control the heat treatment parameters. Some relationships were determined in this research and are discussed below.

The austenitizing temperature is a significant factor affecting the carbides fraction. The center austenitizing temperature (2100°F) results in the highest carbides fraction. On the other hand, the tempering temperature did not affect the carbides fraction significantly, because the tempering temperature range used was high enough to complete all of the carbides nucleation process. Moreover, carbides size was significantly increased by higher tempering temperature due to the fast diffusion of carbon.

Both austenitizing temperature and tempering temperature are significant factors for the hardness of CPM-M4 steel. Higher austenitizing temperature and lower tempering temperature will increase the hardness. The hardness depends more on the matrix structure rather than the carbides phase.

Austenitizing temperature is the only significant factor for the failure strength in the 3-Point bend test. The failure strength depends more on the carbides phase due to the much higher hardness of the carbides. A higher carbides fraction will increase the failure strength in the 3-Point bend test and the maximum carbides fraction can be achieved by controlling the austenitizing temperature. A medium range temperature for austenitizing is preferred.

As for the impact test, austenitizing temperature is also the only significant factor. Higher austenitizing temperature decreases the impact toughness. Moreover, a higher impact toughness corresponds to a higher carbides density. The solid solution strengthening by dissolving of alloy elements in the matrix and the dislocation pinning points created by carbides phase are considered to be the reasons for this relationship. However, higher tempering temperature did not increase the impact toughness, while the hardness dropped significantly. This means that relatively high impact toughness can be achieved without sacrificing hardness. A better balance of hardness and toughness can be achieved through controlling the austenitizing temperature and the tempering temperature, rather than only controlling the tempering process.

From CATRA test, the cutting edge retention of CPM-M4 steel relates to the hardness of materials. Harder materials can provide a better edge retention performance. Because the sharpness retention of blade edge determines the edge retention performance of knife blade, rather than the wear-resistance of

materials. Additionally, a higher edge retention is accompanied by the better initial cutting performance.

8 FUTURE WORK

Based on the results in this study, heat treatment parameters can affect the edged blade performance significantly. However, the specific heat treatment parameter has different effects on different performance. Comparing to the center heat treatment, the percentage change of the performance tested is shown in Figure 28. According to the figure, none of the five heat treatments can achieve highest values in all of the four performance tests. Therefore, the selection of heat treatment parameters should be more specialized, if there is any specific requirements of the final product in the future application. For example, the heat treatments with lower austenitizing temperature can be considered to optimize the impact toughness.

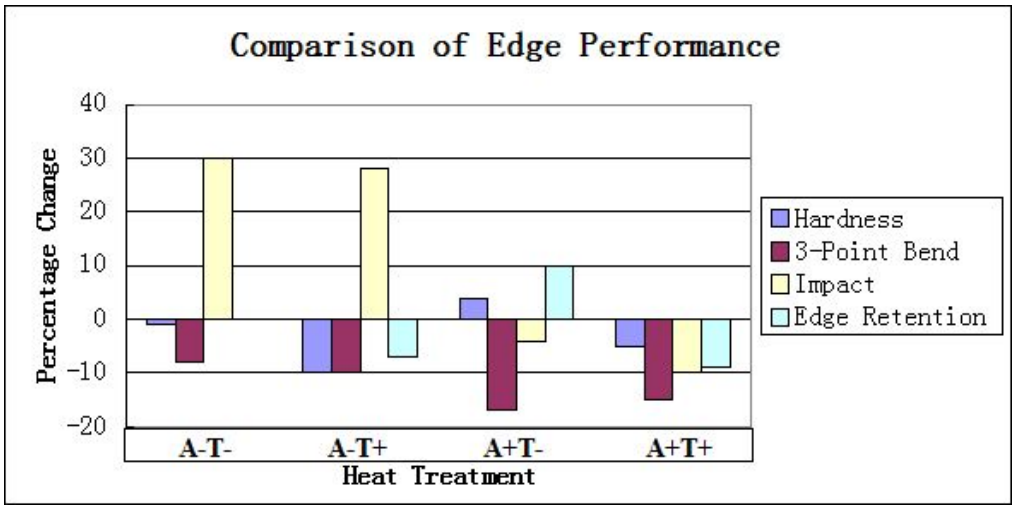

Figure 28. Comparison of edge performance

Although many relationships are defined in this study, there are still some questions to be answered. Future work in this area is justified and is discussed below.

First, the hardness has been defined that it depends more on the matrix structure, however, how the matrix structure determines the hardness is not clear in this study. There are different phase transformations of the matrix during the tempering process, such as bainite formation from the transformation of retained austenite. To get a comprehensive understanding, more techniques need to be applied. EBSD (electron backscatter diffraction) is a recommended technique due to its strong ability in phase identification. Different phases can be quantified by it to better understand the relationship between the hardness performance and the matrix structure. Additionally, micro-hardness testing is necessary to determine the hardness of different phases.

An element analysis of the matrix structure via EDX can provide a more credible data of the alloy elements dissolving process. Additionally, to better understand carbide chemistry and structure, a classification of different carbides needs to be performed using EDX and X-ray diffraction (XRD) techniques.

In the two toughness test, although some relationships were determined, the mechanism of fracture process is not very clear. It is hard to determine the fracture occurred along the grain boundaries or through the grains/carbides. For a better explanation of these relationships, a microstructure examination of the fracture surfaces is needed.

Besides the different techniques, the controlling of heat treatment parameters should be refined. Especially for the impact test, more tempering temperature should be applied to verify our conclusion.

BIBLIOGRAPHY

[1]: “Crucible M4 Datasheet”, Crucible, Retrieved 2005-12

[2]: Robert Wilson, *Metallurgy and Heat Treatment of Tool Steel*, McGRAM-HILL, London, 1975

[3]: Randall M. German, *Powder Metallurgy of Iron and Steel,* John Wiley & Sons, Inc, 1998

[4]: Technical data, Erasteel Company, Research and Development Department, Tour Maine, Montparnasse, 33 avenue du Maine, 75755 Paris Cedex 15

[5]: Jalel Briki, Souad Ben Slima, *A New Continuous Cooling Transformation Diagram for AISI M4 High-Speed Tool Steel*, Journal of Materials Engineering and Performance Volume 17(6) December 2008-869

[6]: C. Garcia, F.G. Caballero, C. Capdevila, and L.F. Alverez, *Application of Delatometric Analysis to the Study of Solid-Solid phase transformations in Steels,* Mater. Character, 2002, 48, p 101-111

[7]: M.C.Payares-Asprino, H.Katsumoto, and S.Liu, *Effect of martensite strat and finish temperature on residual stress development in structure steel welds,* Welding Journal November 2008 Vol.87 p279-289

[8]: F.G. Caballero, L.F. Alverez, C. Capdevila, and C. Garcia de Andres, The Origin of splitting Phenomena in the Martensitic transformation of Stainless Steel, Scripta Mater., 2003, 49, p 315-320

[9]: George Krauss, *Principles of Heat Treatment of Steel*, American Society for Metals, 1980

[10]: Karl-Erik Ehelning, *Steel and its Heat Treatment*, Butterworths London and Boston, 1975

[11]: A.S.M. *Heat Treating of Tool Steels*, Metals Handbook, Vol.2, 8th edition

[12]: “AISI M4 Powdered Metal Datasheet”, Lindquist Steels, Inc.

[13]: “Tooling Alloys Data Sheet CPM REX M4”, ZAPP Materials Engineering, Retrieved 2012-1

[14]:Madeleine Durand-Charre, *Microstructure of Steels and Cast Irons,* Originally published in French, ED. SIRPE, Paris 2003, Translated by James H. Davidson, Springer-Verlag 2004.

[15]: C-B. Ma, T. Ando, D.L. Williamson and G.Krauss, *“Chi-carbides in Tempered High Carbon Martensite”*, Metall. Trans.14A(June 1983), 1033-1045

[16]: G.A.Fontalvo, *Microstructural aspects determining the adhesive of tool steels,* Wear 260 (2006) 1028-1034

[17]: S.-H. Wang, A study of abrasive wear behaviour of laser-clad tool steel coatings, Surface & Coatings Technology 200 (2006) 3446-3458

[18]: ASTM standard E18-14a, *Standard Test Methods for Rockwell Hardness of Metallic Materials*

[19]: T. Horkamani, Sh. Raygan, J. Rassizadehghani, *Comparing microstructure and mechanical properties of AISI D2 steel after bright hardening and oil quenching,* Material and Design 54 (2014) 1049-1055

[20]: Web source from *http://practicalmaintenance.net/?p=1618*

APPENDICES

1. LIST OF ABBREVIATIONS

CPM: Crucible Particle Metallurgy

PM: Powder Metallurgy

SEM: Scan Electron Microscopy

EDX: Energy Dispersive X-ray Spectroscopy

CATRA: Cutlery & Allied Trades Research Association

F.C.C: Face Centered Cubic

B.C.C: Body Centered Cubic

B.C.T: Body Centered Tetragonal

CCT: Continuous Cooling Transformation

Aust: Austenitizing

Temp: Tempering

2. LIST OF SYMBOLS

M_s : Martensite transformation start temperature

M_f : Martensite transformation finish temperature

γ : Iron in F.C.C structure

T_e : Metastable equilibrium temperature for martensite

t: Indentation depth

D: Diffusion coefficient

D_0 : Material constant

Q_d : Activation energy

R: Gas constant

T: Temperature

3. STANDARD SAMPLE PREPARATION PROCEDURES

Four procedures are applied to prepare specimens for SEM imaging: Sectioning, Mounting, Grinding and Polishing, and Etching.

Sectioning:

The specimen size for imaging is limited by the SEM so specimens must be sectioned from the test coupons provided.

A 1.25-inch diameter cylindrical mounting fixture is used to hold specimens for SEM imaging. Since the provided test coupons are 1 inch by 4-inch (width by length) rectangles, appropriately sized specimens must be sectioned from the coupons. The specimens are 0.5x1-inch rectangles. The test coupons and sectioned specimens are 0.125 inches thick. A specimen is cut from a test coupon as shown in Figure 29.

Figure 29. SEM specimen section

To avoid deformation and heat effects during the sectioning procedure, water jet cutting is used. Due to the water jet cutting, the effects of heat can be minimized.

Specimen Mounting for Polishing and Imaging

A mount to hold the steel alloy specimens is fabricated using hot compression mounting. A mount is necessary to hold a specimen during the polishing procedure, and is also needed to hold the specimen during SEM imaging. The fabricated mount is a 1.25 diameter inch cylinder with a height of 0.5 inches. Since conductivity of the specimen is important for SEM imaging, the mount is made from a conductive carbon thermoplastic powder, which will help eliminate charging and drift problems.

There are hot and cold molding processes. The hot procedure is applied since it provides top and bottom surfaces that are close to parallel, which results in a larger area that can be scanned easier during the SEM examination. The SIMPLIMET II machine used for mount fabrication is shown in Figure 30.

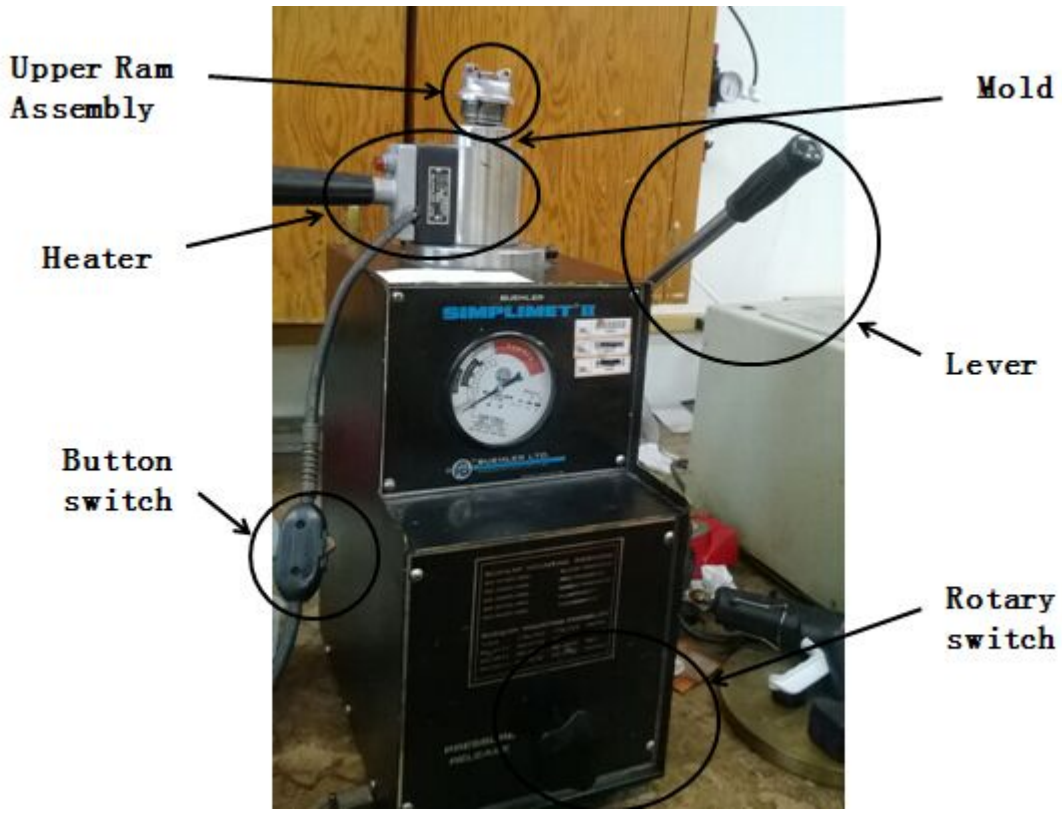

Figure 30. SIMPLIMET II machine used for mounting fabrication

There are six standard steps in the mount fabrication process.

1. Position the specimen inside of the mold and then add the correct amount of carbon mounting powder.

2. Place the upper ram assembly onto the mold. Then rotate in a direction until finger tight with the threads fully engaged.

3. Screw the rotary switch and shake the lever to increase the pressure inside the mold to a correct level.

4. Place the heater outside of the mold and turn on the button switch. Shake the lever to keep the correct pressure since the pressure will fall down during heating. After the pressure is stable wait for 10 minutes.

5. Remove the heater and apply a chill block which is used for cooling the mold until the temperature falls to 225°F. The chill block is shown in Figure 31.

Unscrew the rotary switch to release the pressure. Then unscrew the upper ram assembly. Specimen with a final mount is shown in Figure 32.

Figure 31. Chill block used for cooling

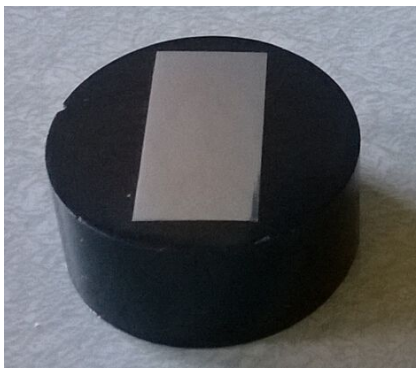

Figure 32. Specimen with a final mount

Specimen Grinding and Polishing

Grinding is used to remove the deformation layer that is formed during previous sample preparation steps and produces a flat surface for microstructure examination. Silicon carbide paper is commonly applied for the grinding procedure.

Typically, grinding starts with 240 grit SiC paper. In our specimen preparation, 4 types of SiC papers with different grit sizes are employed: 240 grit, 320 grit, 400 grit and 600 grit.

Moderate heavy pressure needs to be applied manually during the grinding procedure. The grinding time is 5 minutes with each grinding paper. Also, water is used as a lubricant to flush away removed material and to keep fresh abrasive exposed. The grinding table is shown in Figure 33.

Figure 33. Grinding table

Figure 34. Rotation polishing wheel

Grinding will be followed by a polishing step.

There are three abrasives applied in the polishing procedure: 5 micro alumina abrasives, 0.3 micro α-alumina oxide abrasives and 0.05 micro γ-alumina oxide abrasives. The abrasives are applied to a polishing cloth

during rotation polishing in slurry form. The rotation polishing wheel is shown in Figure 34.

Moderate pressure should be applied manually during rotation polishing. The pressure in the polishing step is lighter than the grinding step. Five minutes of rotation polishing will be employed for each abrasive.

After using each abrasive level the polishing is completed. A cleaning step using an ultrasonic cleaner is then utilized to remove retained abrasives and removed materials.

Specimen Etching

After the grinding and polishing steps, etching is necessary with microscopy to clearly reveal the structure of the material. Different phases will show under the microscope after the etching step.

A proper etchant should be selected for specific materials. In our study, 10% nitric acid is used in the etching step. The etchant should cover the whole surface of the specimens for a proper time.

Since the CPM-M4 steel only contains 4% chromium, the excessive etching should be avoided. 5 seconds is a proper etching time to reveal the general microstructure.

4. ANOVA TABLES

Table 10. ANOVA table for carbides size

Source	*Sum of Squares*	*Df*	*Mean Square*	*F-Ratio*	*P-Value*
MAIN EFFECTS					
A:Aust	1.76271	1	1.76271	1.86	0.173
B:Temp	4.77674	1	4.77674	5.03	0.0249
INTERACTIONS					
AB	0.104648	1	0.104648	0.11	0.7399
RESIDUAL	997.758	1051	0.949341		
TOTAL (CORRECTED)	1004.02	1054			

Only tempering temperature has significant effect at 95% confidence level.

Table 11.ANOVA table for carbides fraction

Source	*Sum of Squares*	*Df*	*Mean Square*	*F-Ratio*	*P-Value*
MAIN EFFECTS					
A:Aust	26.0191	1	26.0191	22.3	0.0015
B:Temp	0.352947	1	0.352947	0.3	0.5973
INTERACTIONS					
AB	0.133141	1	0.133141	0.11	0.7442
RESIDUAL	9.33428	8	1.16678		
TOTAL (CORRECTED)	35.8394	11			

Only austenitizing temperature has significant effect at 95% confidence level.

Table 12. ANOVA table for carbides count

Source	*Sum of Squares*	*Df*	*Mean Square*	*F-Ratio*	*P-Value*
MAIN EFFECTS					
A:Aust	1900.08	1	1900.08	23.7	0.0012
B:Temp	720.75	1	720.75	8.99	0.0171
INTERACTIONS					
AB	60.75	1	60.75	0.76	0.4094
RESIDUAL	641.333	8	80.1667		
TOTAL (CORRECTED)	3322.92	11			

Both austenitizing and tempering temperatures have significant effects at 95% confidence level.

Table 13. ANOVA table for interparticle spacing

Source	*Sum of Squares*	*Df*	*Mean Square*	*F-Ratio*	*P-Value*
MAIN EFFECTS					
A:Aust	9.88264	1	9.88264	44.24	0
B:Temp	4.71811	1	4.71811	21.12	0
INTERACTIONS					
AB	0.381865	1	0.381865	1.71	0.1911
RESIDUAL	234.79	1051	0.223396		
TOTAL (CORRECTED)	248.705	1054			

Both austenitizing and tempering temperature have significant effects at 95% confidence level.

Table 14. ANOVA table for hardness test

Source	*Sum of Squares*	*Df*	*Mean Square*	*F-Ratio*	*P-Value*
MAIN EFFECTS					
A:Aust	241.802	1	241.802	1117.09	0.0000
B:Temp	826.562	1	826.562	3818.58	0.0000
INTERACTIONS					
AB	0.0025	1	0.0025	0.01	0.9146
RESIDUAL	20.78	96	0.216458		
TOTAL (CORRECTED)	1089.15	99			

Both austenitizing and tempering temperature have significant effects at 95% confidence level.

Table 15. ANOVA table for 3-Point Bend test

Source	*Sum of Squares*	*Df*	*Mean Square*	*F-Ratio*	*P-Value*
MAIN EFFECTS					
A:Aust	21,409.624	1	21,409.624	10.203	0.00565
B:Temp	7.351	1	7.351	0.0035	0.95353
INTERACTIONS					
AB	2,785.645	1	2,785.645	1.32754	0.26617
RESIDUAL	33,573.726	16	2,098.358		
TOTAL (CORRECTED)	57,776.346	19	3,040.86		

Only austenitizing temperature has significant effect at 95% confidence level.

Table 16. ANOVA table for impact test

Source	*Sum of Squares*	*Df*	*Mean Square*	*F-Ratio*	*P-Value*
MAIN EFFECTS					
A:Impact_M4.Aust	51.8903	1	51.8903	32.66	0.0000
B:Impact_M4.Temp	0.651966	1	0.651966	0.41	0.5309
INTERACTIONS					
AB	0.250656	1	0.250656	0.16	0.6965
RESIDUAL	25.4238	16	1.58899		
TOTAL (CORRECTED)	78.2167	19			

Only austenitizing temperature has significant effect at 95% confidence level.

Table 17. ANOVA table for comparison between average carbides sizes of the center heat treatment and the responding as-quenched sample

Source	*Sum of Squares*	*Df*	*Mean Square*	*F-Ratio*	*P-Value*
Between groups	0.345166	1	0.345166	0.24	0.6235
Within groups	685.271	479	1.43063		
Total (Corr.)	685.616	480			

There is no significant difference between the carbides sizes of the center heat treatment and the responding as-quenched sample at 95% confidence lever.

Table 18. ANOVA table for operator comparison in the hardness test

Source	*Sum of Squares*	*Df*	*Mean Square*	*F-Ratio*	*P-Value*
Between groups	3.61412	1	3.61412	0.55	0.4576
Within groups	2765.51	423	6.53784		
Total (Corr.)	2769.12	424			

There is no significant difference between different operators at 95% confidence lever.